Time-resolved parameterization of aperiodic and periodic brain activity

Luc E. Wilson[1], Jason da Silva Castanheira [1], Sylvain Baillet[1]†

[1] McConnell Brain Imaging Centre, Montreal Neurological Institute, McGill University, Montreal, QC H3A 2B4, Canada

† Corresponding authors: sylvain.baillet@mcgill.ca.

Abstract

Macroscopic neural dynamics comprise both aperiodic and periodic components. Recent advances in parameterizing neural power spectra offer practical tools for evaluating these features separately. Although neural signals vary dynamically and express non-stationarity in relation to ongoing behaviour and perception, current methods yield static spectral decompositions. Here, we introduce Spectral Parameterization Resolved in Time (SPRiNT) as a novel method for decomposing complex neural dynamics into periodic and aperiodic spectral elements in a time-resolved manner. First, we demonstrate, with naturalistic synthetic data, SPRiNT's capacity to reliably recover time-varying spectral features and emphasize SPRiNT's specific strengths over other time-frequency parameterization approaches based on wavelets. Second, we use SPRiNT to further illustrate how aperiodic spectral features fluctuate across time in resting-state electroencephalography (n = 178) and relate changes in aperiodic parameters to participants' demographics and behaviour. Lastly, we use SPRiNT to demonstrate aperiodic dynamics related to movement behaviour in intracranial recordings in rodents. We foresee SPRiNT responding to growing neuroscientific interests in the parameterization of time-varying neural power spectra and advancing the quantitation of complex neural dynamics at the natural time scales of behaviour.

Keywords: aperiodic, periodic, time-resolved, parameterization, power spectra, neural oscillations, electrophysiology.

Significance Statement

The new method and reported findings address a growing interest in neuroscience for research tools that can reliably decompose brain activity at the mesoscopic scale into interpretable components. We show that the new approach proposed herein is capable of tracking transient, dynamic spectral (aperiodic and periodic) components across time, both in synthetic simulated and experimental data. We anticipate that this novel technique, SPRiNT, will enable new neuroscience inquiries that reconcile multifaceted neural dynamics with complex behaviour.

Introduction

The brain constantly expresses a repertoire of complex dynamics related to behaviour in health and disease. Neural oscillations, for instance, are rhythmic components of brain activity that emerge from a background of aperiodic fluctuations recorded with a range of electrophysiological techniques at the mesoscopic scale (Buzsáki, 2006). Brain oscillations and their dynamics have been causally linked to individual behaviour and cognition (Albouy et al., 2017), and shape brain responses to sensory stimulation (Samaha et al., 2020).

Current methods for measuring the time-varying properties of neural fluctuations include several time-frequency decomposition techniques such as Hilbert, wavelet, and short-time Fourier signal transforms (Bruns, 2004; Cohen, 2014). Following spectral decomposition, oscillatory activity within the empirical bands of electrophysiology manifests as peaks of signal power (Buzsáki and Watson, 2012; Cohen, 2014). However, time-resolved signal power decompositions do not explicitly account for the presence of aperiodic signal components, which challenge both the detection and the interpretability of spectral peaks as genuine periodic signal elements (Donoghue et al., 2020). This is critical as aperiodic and periodic components of neural activity represent distinct, although possibly interdependent physiological mechanisms (Gao et al., 2017).

Aperiodic neural activity is characterized by a reciprocal distribution of power with frequency (1/f), which can be parameterized with two scalars: *exponent* and *offset*. These parameters are physiologically meaningful: current constructs consider the offset as reflecting neuronal population spiking, and the exponent as related to the integration of synaptic currents (Voytek & Knight, 2015) and reflecting the balance between excitatory (E) and inhibitory (I) currents (i.e., the larger the exponent, the stronger the inhibition; Chini et al., 2021; Gao et al., 2017; Waschke et al., 2021). Aperiodic neural activity is ubiquitous throughout the brain (He,

2014); it differentiates healthy aging (Cellier et al., 2021; Donoghue et al., 2020; Ostlund et al., 2022; Schaworonkow and Voytek, 2021; Voytek et al., 2015), and is proposed as a potential marker of neuropsychiatric conditions (Molina et al., 2020) and epilepsy (van Heumen et al., 2021). Though the study of aperiodic neural activity has recently advanced, unanswered questions remain about its functional relevance, which requires an expanded toolkit to track their evolution across time and the broadest possible expressions of behaviour.

One little studied aspect of aperiodic activity is its fluctuations, both spontaneously over time, and with task and mental states. Baseline normalization is a common approach to compensate for aperiodic contributions to time-frequency decompositions (Cohen, 2014), with the underlying assumption, however, that characteristics of aperiodic activity (exponent and offset) remain unchanged throughout the data length—an assumption that is challenged by recent empirical data (Van Heumen et al., 2021; Waschke et al., 2021). Akin to the motivations behind aperiodic/periodic spectral parameterization and signal decomposition techniques (Donoghue et al., 2020, Wen & Liu, 2016), undetected temporal variations of the neural spectrogram may conflate fluctuations in aperiodic activity with modulations of oscillatory signals, hence distorting data interpretation (Donoghue et al., 2020). Recent methodological advances have contributed practical tools to decompose and parameterize the neural power spectrum into aperiodic (scale-free, 1/f) and narrow-band periodic components (spectral peaks of certain widths; Donoghue et al., 2020; Wen & Liu, 2016; He, 2014). One such practical tool (*specparam*) sequentially fits aperiodic and oscillatory parametric components to the empirical neural power spectrum (Donoghue et al., 2020). The resulting model for the aperiodic component is represented with exponent and offset scalar parameters, and periodic elements are modelled with a series of Gaussian functions characterised with three scalar parameters (centre frequency, amplitude, and standard deviation).

Specparam accounts for static spectral representations and has yet to be extended to account for the non-stationary contents of neural time series.

We introduce SPRiNT (Spectral Parameterization Resolved in Time) as a novel approach to identify and model dynamic shifts in aperiodic and periodic brain activity, yielding a time-resolved parameterization of empirical neural spectrograms. We validate the method with an extensive set of naturalistic simulations of neural data, with benchmark comparisons to parameterized wavelet signal decompositions. Using SPRiNT, we also show that aperiodic fluctuations of the spectrogram can be related to meaningful behavioural and demographic variables from human EEG resting-state data and electrophysiological recordings from free-moving rodents.

Results

SPRiNT consists of the following methodological steps. First, short-time Fourier transforms (STFT) are derived from overlapping time windows that slide over data time series. Second, the resulting STFT coefficients are averaged over consecutive time windows to produce a smooth estimate of the power spectral density of the recorded data. Third, the resulting spectrum is parameterized into aperiodic and periodic components using specparam (see Methods). As the procedure is repeated over the entire length of the data, SPRiNT produces a time-resolved parameterization of the data's spectrogram (Figure 1A). The resulting parameters can then be compiled into time-frequency representations for visualization and further derivations. A fourth step consists of an optional post-processing procedure meant to prune outlier transient manifestations of periodic signal components (Supplemental Figure S1).

We generated a total of 20,000 naturalistic synthetic neural time series with non-stationary aperiodic and periodic signal components using scripts adapted from the NeuroDSP toolbox (Cole et al., 2019) with MATLAB (R2020a; Natick, MA). We first tested SPRiNT's ability to detect and track transient and chirping periodic elements (with time-changing aperiodic components) and benchmarked its performance against parametrized wavelet signal decompositions (Figure 1B). A second validation challenge focused on simulations derived from randomly generated sets of realistic aperiodic and periodic parameters; this challenge served to assess SPRiNT's performance across naturalistic heterogenous signals (Figure 1C; see Methods). Further below, we describe the application of SPRiNT to a variety of empirical data from human and rodent electrophysiology.

Methods benchmarking (synthetic data).

We first simulated 10,000 time series (60 s duration) with aperiodic components transitioning linearly between t=24s and t=36 s, from an initial exponent of 1.5 Hz and offset of -2.56 [arbitrary units, a.u.] to a final exponent of 2.0 Hz and offset of -1.41 a.u. The periodic components of the simulated signals included transient activity in the alpha band (centre frequency: 8 Hz; amplitude: 1.2 a.u.; standard deviation: 1.2 Hz) occurring between 8-40 s, 41-46 s, and 47-52 s, and a down-chirping oscillation in the beta band (centre frequency decreasing from 18 to 15 Hz; amplitude: 0.9 a.u.; standard deviation: 1.4 Hz, between 15-25 s (Figure 1B). We applied SPRiNT on each simulated time series, post-processed the resulting parameter estimates to remove outlier transient periodic components, and derived goodness-of-fit statistics of the SPRiNT parameter estimates with their ground-truth values. We compared SPRiNT's performances to the parameterization of temporally smoothed spectrograms obtained from Morlet wavelets time-frequency decompositions of the simulated time series (smoothed using a 4 s Gaussian kernel, standard

deviation = 1 s). We refer to this approach as *wavelet-specparam* (see Methods). We assessed the respective performances of SPRiNT and *wavelet-specparam* with measures of Mean Absolute Error (MAE) on their respective estimates of spectrogram time-frequency profiles and of the parameters of their a/periodic components across time.

Overall, we found that SPRiNT spectrogram models were closer to ground truth (MAE = 0.04, SEM [standard error of the mean] = 3.0×10^{-5}) than those from *wavelet-specparam* (MAE = 0.58, SEM = 5.1×10^{-6}; Figure 2a). The data showed marked differences in performance between SPRiNT and *wavelet-specparam* in the parametrization of aperiodic components (error on aperiodic spectrogram: *wavelet-specparam* MAE = 0.60, SEM = 6.7×10^{-6}; SPRiNT MAE = 0.05, SEM = 4.1×10^{-5}). The performances of the two methods in parametrizing periodic components were strong and similar (*wavelet-specparam* MAE = 0.05, SEM = 4.0×10^{-5}; SPRiNT MAE = 0.02, SEM = 2.7×10^{-5}).

SPRiNT errors on exponents (MAE = 0.11, SEM = 7.8×10^{-5}) and offsets (MAE = 0.14, SEM = 1.1×10^{-4}) were substantially less that those from *wavelet-specparam* (exponent MAE = 0.19, SEM = 1.5×10^{-5}; offset MAE = 0.79, SEM = 2.7×10^{-5}; Figure 2A). SPRiNT detected periodic alpha activity with similar sensitivity (99% at time bins with maximum peak amplitude) but higher specificity (96%) than *wavelet-specparam* (98% sensitivity, 63% specificity). SPRiNT estimates of alpha peak parameters were also closer to ground truth (centre frequency, amplitude, bandwidth MAE [SEM] = 0.35 [3.2×10^{-4}] Hz, 0.21 [1.7×10^{-4}] a.u., 0.42 [3.8×10^{-4}] Hz, respectively) than *wavelet-specparam*'s (MAE [SEM] = 0.43 Hz [4.5×10^{-5}], 0.21 [2.0×10^{-5}] a.u., 0.61 [5.7×10^{-5}] Hz, respectively; Figure 2C). SPRiNT detected and tracked down-chirping beta periodic activity with higher sensitivity (95% at time bins with maximum peak amplitude) and comparable specificity (99%) to *wavelet-specparam* (67% sensitivity, 99% specificity). SPRiNT's estimates of beta peak

parameters were also closer to ground truth (centre frequency, amplitude, bandwidth MAE = 0.47 [3.9×10^{-4}] Hz, 0.18 [1.5×10^{-4}] a.u., 0.48 [4.0×10^{-4}] Hz, respectively) than with *wavelet-specparam* (centre frequency, amplitude, bandwidth MAE = 0.50 [8.3×10^{-5}] Hz, 0.14 [1.9×10^{-5}] a.u., 1.05 [8.1×10^{-5}] Hz, respectively; Figure 2C). We noted that both methods tended to overestimate peak bandwidths (Supplemental Figure S2), and the effect was more pronounced with *wavelet-specparam* (Figure 2C). We report raw SPRiNT performances prior to the removal of outlier peaks in Supplemental Materials.

Generalization of SPRiNT across generic aperiodic and periodic fluctuations (synthetic data).

We simulated 10,000 additional time series consisting of aperiodic and periodic components, whose parameters were sampled continuously from realistic ranges (Figure 1C). The generators of each trial time series comprised i) one aperiodic component whose exponent and offset parameters were shifted linearly over time, and ii) 0 to 4 periodic components (see Methods for details). SPRiNT, followed by outlier peak post-processing, recovered 71% of the simulated periodic components, with 84% specificity (72% sensitivity and 67% specificity prior to outlier removal as shown in Supplemental Figure S3). Aperiodic exponent and offset parameters were recovered with MAEs of 0.12 and 0.15, respectively. The centre frequency, amplitude, and frequency width of periodic components were recovered with MAEs of 0.49, 0.24, and 0.50, respectively (Figure 3B). We evaluated whether the detection and accuracy of parameter estimates of periodic components depended on their frequency and amplitude (Figure 3C). The synthetized data showed that overall, SPRiNT accurately detects up to two simultaneous periodic components (Figure 3D). We also found that periodic components of lower frequencies were more challenging to detect (Figure 3C

& 3D) because their peak spectral component tended to be masked by the aperiodic (1/f) component of the power spectrum. Model fit errors (MAE = 0.31) varied significantly with the number of simultaneous periodic components, but this effect was small (β = -0.0004, SE = 6.5x 10^{-6}, 95% CI [-0.0004 0.0004]; R^2 = 0.003; Figure 3E).

Aperiodic and periodic fluctuations in resting-state EEG dynamics with eyes-closed, eyes-open behaviour (empirical data).

We applied SPRiNT to resting-state EEG data from the openly available LEMON dataset (Babayan et al., 2019). Participants (*n* = 178) were instructed to open and close their eyes (alternating every 60 s). We used *Brainstorm* (Tadel et al., 2011) to preprocess EEG time series from electrode Oz and obtain time-frequency decompositions with Morlet wavelets (with default parameters, see Methods). We ran SPRiNT on the same preprocessed EEG time series.

As expected, SPRiNT identified time-varying fluctuations of both aperiodic and periodic (alpha range, 6-14 Hz) components of the Oz spectrogram as participants opened or closed their eyes (Figure 4A and Supplemental Figure S4). These changes in the alpha band were also visible in the wavelet spectrogram. We found the wavelet estimate of alpha band signal power to be associated with the experimental condition (β = -1.99, SE = 0.30, 95% CI [-2.61, -1.42]; Bayes factor BF = 5.00×10^{-11}; Supplemental Table S1). As expected, time points of reduced alpha power predicted that participants had their eyes open.

We ran a similar logistic regression model with SPRiNT parameter estimates as fixed effects (mean and standard deviation of alpha centre frequency, alpha power, and the aperiodic exponent across time). We found a significant effect of mean alpha power (β = -6.57, SE = 0.93, 95% CI [-8.51, -4.84]), standard deviation of alpha power (β = 5.43, SE = 1.99, 95% CI [1.62,

9.46]), and mean aperiodic exponent (β = 2.52, SE = 0.52, 95% CI [1.52, 3.59]) as predictors of eyes-open vs. eyes-closed behaviour (Supplemental Table S2). According to this model, lower alpha power, larger aperiodic exponents, and stronger fluctuations of alpha-band activity over time are signatures of the eyes-open resting-state. A Bayes factor analysis confirmed the evidence of effects from mean alpha power (BF = 9.97×10^{-14}) and mean aperiodic exponent (BF = 2.20×10^{-4}), and indicated anecdotal evidence against the variability of alpha power (BF = 1.80; Supplemental Figure S5). In summary, both wavelet and SPRiNT analyses confirmed alpha power as a neurophysiological marker of eyes-closed vs. eyes-open behavior. Yet SPRiNT's spectrogram parametrization was uniquely able to reveal time-varying changes of aperiodic components related to eyes-closed vs. eyes-open behavior.

Prediction of biological age group from aperiodic and periodic components of the resting-state EEG spectrogram (empirical data).

Using the same dataset, we tested the hypothesis that SPRiNT parameter estimates are associated with participants' age group (i.e., younger [*n* = 121] vs older [*n* = 57] adults). Extant literature reports slower alpha rhythms and smaller aperiodic exponents in healthy aging (Donoghue et al., 2020). We performed a logistic regression based on SPRiNT parameter estimates of the mean and standard deviation of alpha centre frequency, alpha power, and aperiodic exponent as fixed effects in the eyes-open condition. We found significant effects of mean aperiodic exponent (β = -3.30, SE = 0.75, 95% CI [-4.85, -1.90]) and standard deviation of alpha centre frequency (β = 1.27, SE = 0.54, 95% CI [0.24, 2.35]; Supplemental Table S3). We therefore found using SPRiNT that the EEG spectrogram of older participants was flatter and expressed stronger time-varying fluctuations of alpha-peak centre frequency. A Bayes factor analysis showed strong evidence for the effect of

the aperiodic exponent (BF = 3.82×10^{-5}) and for the variability of the alpha band peak frequency (BF = 0.24; Supplemental Figure S6).

We replicated the same analysis with the data in the eyes-closed condition. We found with SPRiNT that mean aperiodic exponent (β = -4.25, SE = 0.83, 95% CI [-6.01, -2.72]) and mean alpha centre frequency (β = -0.68, SE = 0.26, 95% CI [-1.22, -0.18]) were predictors of participants' age group, with older participants again showing a flatter spectrum and a slower alpha peak (lower centre frequency; Supplemental Table S4). A Bayes factor analysis provided strong evidence for the effect of mean aperiodic exponent (BF = 1.80×10^{-7}) and strong evidence for the effect of mean alpha centre frequency (BF = 0.13; Supplemental Figure S7).

Using the wavelet spectrogram alternative, we found that mean alpha power was the only discriminant feature for age group in the eyes-closed condition (β = -1.14, SE = 0.38, 95% CI [-1.92, -0.41]; Supplemental Table S5). Contrasting with SPRiNT's present findings, the effect of age was confined to alpha power using wavelet spectrograms. Because wavelet spectrograms are not readily decomposed into aperiodic and periodic components, their findings could be alternatively interpreted as caused by age-related effects on aperiodic exponent or alpha-peak centre frequency (as discussed by Scally et al., 2018). There was no wavelet-based predictor of age group in the eyes-open condition (Supplemental Table S6).

Transient changes in aperiodic brain activity associated with rodent locomotor behaviour (empirical data).

We used intracranial data from two Long-Evans rats recorded in layer 3 of entorhinal cortex while they moved freely along a linear track (Mizuseki et al., 2009; https://crcns.org). Rats travelled alternatively to either end of the track to receive a water reward, resulting in behaviours of

recurring bouts of running and resting. Power spectral density estimates revealed substantial power increases below 20 Hz during rest with respect to movement (Figure 5; Samiee & Baillet, 2017). We therefore tested for the possible expression of two alternating modes of aperiodic neural activity associated with each behaviour. SPRiNT parameterization found in the two subjects that resting bouts were associated with larger aperiodic exponents and more positive offsets than during movement bouts (Supplemental Figure S9). We ran SPRiNT parameterizations over eight-second epochs proximal to transitions between movement and rest, and observed dynamic shifts between aperiodic modes associated with behavioural changes (Figure 5). We found that the periodic features of the recordings were non-sinusoidal and therefore should not be parametrized with the methods discussed herein (Donoghue et al., 2021; Supplemental Figure S8).

Discussion

We introduce SPRiNT as a new method to parameterize dynamic fluctuations in the spectral contents of neural time series. SPRiNT extends recent practical tools that determine aperiodic and periodic parameters from static power spectrum density estimates of neural signals to their spectrograms. Aperiodic spectral components may confound the detection and interpretation of narrow-band power changes as periodic, oscillatory signal elements. Given the scientific prominence of measures of neural oscillations in (causal) relation to behaviour (e.g., Albouy et al., 2017) and clinical syndromes (e.g., Ostlund et al., 2021), it is essential that their characterization in time and frequency be contrasted with that of the underlying aperiodic background activity at the natural time scale of behaviour and perception.

SPRiNT expands the neural spectrogram toolkit

Recent empirical studies show that the spectral distribution of neural signal power with frequency can be decomposed into low-dimensional aperiodic and periodic components (Donoghue et al., 2020), and that these latter are physiologically (Gao et al., 2019), clinically (Molina et al., 2020; Van Heumen et al., 2021), and behaviourally (Ouyang et al., 2020; Waschke et al., 2021) meaningful.

SPRiNT extends the approach to the low-dimensional time-resolved parameterization of neural spectrograms. The method combines the simplicity of the *specparam* spectral decomposition approach with the computational efficiency of short-time Fourier transforms across sliding windows. The present results demonstrate its technical concept and indicate that SPRiNT unveils meaningful additional information from the data, beyond established tools such as wavelet time-frequency decompositions.

Using realistic simulations of neural time series, we demonstrate the strengths and current limitations of SPRiNT. We show that SPRiNT decompositions provide a comprehensive account of the neural spectrogram (Figure 2A), tracking the dynamics of periodic and aperiodic signal components across time (Figure 2B and Supplemental Figure S2). We note that the algorithm performs optimally when the data features narrow-band oscillatory components that can be characterized as spectral peaks (Figure 3C). The algorithm performs best when the data contains two or fewer salient oscillatory components concurrently (Figure 3D). We found that these current limitations are inherent to *specparam*, which is challenged by the dissociation of spectral peaks from background aperiodic activity at the lower edge of the power spectrum (Donoghue et al., 2020)

298 Practical mitigation techniques have been proposed to account for the presence of
299 background aperiodic activity when estimating narrow-band signal power changes. For instance,
300 baseline normalization is a common approach used to isolate event-related signals and prepare
301 spectrograms for comparisons across individuals (Cohen, 2014). However, the resulting relative
302 measures of event-related power increases or decreases do not explicitly account for the fact that
303 behaviour or stimulus presentations may induce rapid changes in aperiodic activity. Therefore,
304 baseline normalization followed by narrow-band analysis of power changes is not immune to
305 interpretation ambiguities when aperiodic background activity also changes dynamically. Further,
306 the definition of a reference baseline can be inadequate for some study designs, as exemplified
307 herein with the LEMON dataset.
308

309 **SPRiNT decomposition of EEG data tracks and predicts behaviour & demographics**

310 We found in the LEMON dataset that measuring narrow band power changes without accounting
311 for concurrent variations of the aperiodic signal background challenges the interpretation of effects
312 manifested in the spectrogram (Scally et al., 2018). SPRiNT enables this distinction, showing that
313 both periodic and aperiodic changes in neural activity are associated with age and behaviour. We
314 found strong evidence for decreases in alpha-peak power and increases in aperiodic exponent
315 during eyes-open resting-state behaviour (compared to eyes-closed; Figure 4A). However, it
316 remains unclear whether these effects are independent or related; a recent analysis of the same
317 dataset showed that the amplitude of alpha oscillations around a non-zero mean voltage influence
318 baseline cortical excitability (Studenova et al., 2021)—an effect observable in part through
319 variations of the aperiodic exponent (Gao et al., 2017). We also observed both slower alpha-peak
320 centre frequencies and smaller aperiodic exponents in the older age group (Figure 4B), in

agreement with previous literature on healthy aging (Cellier et al., 2021; Donoghue et al., 2020; Ostlund et al., 2022; Schaworonkow & Voytek, 2021).

We also emphasize how the variability of spectral parameters may relate to demographic features, as shown with SPRiNT's prediction of participants' age from the variability of alpha-peak centre frequency over the duration of the recording (Figure 4C). Previous studies explored similar effects of within-subject variability of alpha peak centre frequency (Haegens et al., 2014) and their clinical relevance (Larsson & Kostov 2005). These findings augment the recent evidence that neural spectral features are robust signatures proper to an individual (da Silva Castanheira et al., 2021) and open the possibility that their temporal variability be neurophysiologically significant.

We also report time-resolved fluctuations in aperiodic activity related to behaviour in freely moving rats (Figure 5). SPRiNT aperiodic parameters highlight larger spectral exponents in rats during rest than during movement. Time-resolved aperiodic parameters can also be tracked with SPRiNT as subjects transition from periods of movement to rest and vice-versa. The smaller aperiodic exponents observed during movement may be indicative of periods of general cortical disinhibition (Gao et al., 2017). Previous work on the same data has associated how locomotor behavior is associated with changes in amplitude and centre frequency of entorhinal theta rhythms (Mizuseki et al., 2009; Samiee & Baillet, 2017). Strong theta activity may challenge the estimation of aperiodic parameters (Gao et al., 2017). The nature and function of the changes in aperiodic exponent with behaviour detected with SPRiNT demonstrated in the present data remain to be determined, but these observations support the notion that aperiodic background neural activity changes in relation to a variety of contexts and subject types

(Donoghue et al., 2020; Gao et al., 2017; Molina et al., 2020; Ostlund et al., 2021; Pathania et al., 2021; Waschke et al., 2021; van Heumen et al., 2021).

Future directions

We used the short-time Fourier transform as the underlying time-frequency decomposition technique for SPRiNT. A major asset of STFT is computational efficiency, but with sliding time windows of fixed duration, the method demonstrates the trade-off between temporal specificity and frequency resolution (Cohen, 2014). Combining *specparam* with STFT yields rapid extraction of spectral parameters from time-frequency data. In principle, spectral parameterization should be capable of supplementing any time-frequency decomposition technique, such as wavelet transforms (Pietrelli et al., 2021), though at the expense of significantly greater computational cost. However, we have shown with the *wavelet-specparam* method herein that parameterizing wavelet transforms does not accurately recover aperiodic signal components. Further, at the levels of temporal smoothing necessary to reduce parameter estimation error to similar levels as SPRiNT's (4-s Gaussian kernel; Figure 2), the high temporal sampling of wavelet spectral parameterization becomes redundant. The advantages to such an approach over parameterized STFTs (i.e., SPRiNT) are unclear, because parameter estimates are accurate even with relatively low time and frequency resolutions (0.5 s and 1 Hz as shown in Figures 2 & 3). Another alternative to STFT would be the *superlet* approach (Moca et al., 2021) designed to preserve a fixed resolution across time (number of cycles) and frequency. Combining *superlets* with *specparam* is to be explored, although reduced computational cost remains a practical benefit of STFT.

SPRiNT has some limitations similar to *specparam* (Donoghue et al., 2020). For example, the determination of periodic component parameters (number of peaks, peak amplitude) may be

prone to overfitting the number of peaks in the data. Here, we propose a pragmatic approach to this issue with a postprocessing step that consists in pruning the outcome of original SPRiNT parameters from unlikely, transient periodic components (Supplemental Figure 1). Identifying the most parsimonious number of oscillatory peak components in the data (via model selection e.g., via Bayesian Information Criteria; Schwarz, 1978) may be an approach worth exploring in that respect.

In conclusion, the SPRiNT algorithm enables the parameterization of the neural spectrogram. We validated the time tracking of periodic and aperiodic spectral features with a large sample of ground-truth synthetic time series, and empirical data from the human resting-state, and rodent intracranial electrophysiological recordings. We showed that SPRiNT provides estimates of dynamic fluctuations of aperiodic and periodic neural activity that are related to meaningful demographic or behavioural outcomes. We anticipate that SPRiNT and future related developments will augment the neuroscience toolkit and enable new advances in the characterization of complex neural dynamics.

Methods

SPRiNT runs on individual time series and returns a parameterized time-frequency representation of the spectrogram. The algorithm first derives short-time fast Fourier transforms (FFTs) over time windows that slide on the time series. Second, the modulus of FFT coefficients is averaged over *n* consecutive time windows to produce smoothed power spectral density (PSD) estimates at each time bin. Third, each of the resulting PSDs are parameterized into periodic and aperiodic components, using the *specparam* algorithm. A fourth optional step consists of the removal of outlier periodic components from the raw SPRiNT spectrograms. We developed SPRiNT as a plug-in library that interoperates with *Brainstorm* (Tadel et al., 2011).

Parameterization of short-time FFT

Short-time Fourier transforms are computed iteratively on sliding time windows (default window length = 1 s; tapered by a Hann window) using MATLAB's Fast Fourier Transform (FFT; R2020a; Natick, MA). Each window overlaps with its nearest neighbours (default overlap = 50%). The modulus of Fourier coefficients of the running time window is then averaged locally with those from preceding and following time windows, with the number of time windows included in the average, n, determined by the user (default is $n = 5$; Figure 1A). The resulting periodogram is then parameterized with *specparam*. The resulting spectrogram is time-binned based on time points located at the centre of each sliding time window.

Tracking periodic and aperiodic components across time

We used the MATLAB implementation of *specparam* in *Brainstorm* (Tadel et al., 2011), adapted from the original Python code (Version 1.0.0) by Donoghue et al. (2020). The aperiodic component

of the power spectrum is typically represented using two parameters (exponent and offset); an additional knee parameter is added when a bend is present in the aperiodic component (Donoghue et al., 2020; Gao et al., 2020). Periodic components are parameterized as peaks emerging from the aperiodic component using Gaussian functions controlled with three parameters (mean [centre frequency], amplitude, and standard deviation).

For algorithmic speed optimization purposes, in each iteration of *specparam* across time, the optimization of the aperiodic exponent is initialized from its *specparam* estimate from the preceding time bin. All other parameter estimates are initialized using the same data-driven approaches as *specparam* (Donoghue et al., 2020).

Pruning of periodic component outliers

We derived a procedure to remove occasional peaks of periodic activity from parameterized spectrograms and emphasize expressions of biologically plausible oscillatory components across successive time bins. This procedure removes peaks with fewer than a user-defined number of similar peaks (by centre frequency; default = 3 peaks within 2.5 Hz) within nearby time bins (default = 6 bins). This draws from observations in synthetic data that non-simulated peaks are parameterized in isolation (few similar peaks in neighbouring time bins; Supplemental Figure S1). Aperiodic parameters are refit at time bins where peaks have been removed, and models are subsequently updated to reflect changes in parameters. This post-processing procedure is applied on all SPRiNT outputs shown but remains optional (albeit recommended).

Study 1: Time Series Simulations

We simulated neural time series using in-house code based on the NeuroDSP toolbox (Cole et al., 2019) with MATLAB (R2020a; Natick, MA). The time series combined aperiodic with periodic components (Donoghue et al., 2020). Each simulated 60-s time segment consisted of white noise sampled at 200 Hz generated with MATLAB's coloured noise generator (R2020a; Natick, MA). The time series was then Fourier-transformed (frequency resolution = 0.017 Hz) and convolved with a composite spectrogram of simulated aperiodic and periodic dynamics (temporal resolution = 0.005 s). The final simulated time series was generated as the linear combination of cosines of each sampled frequency (with random initial phases), with amplitudes across time corresponding to the expected power from the spectrogram.

Simulations of transient and chirping peak components

The aperiodic exponent was initialized to 1.5 Hz^{-1} and increased to 2.0 Hz^{-1}, offset was initialized to -2.56 a.u. and increased to -1.41 a.u.; both linearly increasing between the 24 s and 36 s time stamps of the time series. Periodic activity in the alpha band (centre frequency = 8 Hz, amplitude = 1.2 a.u., standard deviation = 1.2 Hz) was generated between time stamps 8s and 40 s, as well as between 41-46 s and 47-52 s. Periodic activity in the beta band (centre frequency = 18 Hz, amplitude = 0.9 a.u., standard deviation = 1.4 Hz) was generated between 15-25 s and down-chirped linearly from 18-15Hz between 18-22 s. Peak amplitude was calculated as the relative height above the aperiodic component at every sampled frequency and time point. All amplitudes of periodic activity were tapered by a Tukey kernel (cosine fraction = 0.4). Aperiodic and periodic parameters (and their dynamics) were combined to form a spectrogram of simulated activity.

All simulations (n = 10,000) were unique as each was generated from a unique white-noise time series seed, and the cosine waves to simulate periodic components were each assigned a random initial phase.

Each simulated time series was analyzed with SPRiNT using 5x1s sliding time windows with 50% overlap (frequency range: 1-40 Hz). Settings for *specparam* were set as: peak width limits: [0.5 6]; maximum number of peaks: 3; minimum peak amplitude: 0.6 a.u.; peak threshold: 2.0 standard deviations; proximity threshold: 2 standard deviations; aperiodic mode: fixed. Settings for peak post-processing were set as: number of neighbouring peaks: 3; centre frequency: 2.5 Hz; time bin: 6 bins (= 3 s). Periodic alpha activity was identified using the highest amplitude peak parameterized in each time bin between 5.5-10.5 Hz, while periodic beta activity was identified using the highest amplitude peak in each time bin between 13.5-20.5 Hz.

We also parameterized Morlet wavelet spectrograms of each simulated time series using *specparam* (Donoghue et al., 2020; MATLAB version). Wavelet transforms were computed with *Brainstorm* (Tadel et al., 2011; 1-40 Hz, in 1 Hz steps) using default settings (central frequency = 3 Hz, FWHM = 1 s). Before parameterizing wavelet transforms, we applied a 4 s temporal smoothing filter (Gaussian kernel, standard deviation = 1 s; time range: 3.5-56.5 s, in 0.005 s steps) to increase signal-to-noise ratio (results prior to this step are shown for the first 1,000 simulations in Supplemental Materials). Settings for *specparam* were set as: peak width limits: [0.5 6]; maximum number of peaks: 3; minimum peak amplitude: 0.6 a.u.; peak threshold: 2.0 standard deviations; proximity threshold: 2 standard deviations; aperiodic mode: fixed. Periodic alpha activity was identified using the highest amplitude peak parameterized in each time bin between 5.5-10.5 Hz. Periodic beta activity was identified using the highest amplitude peak in each time bin between 13.5-20.5 Hz.

Model fit error was calculated as the mean absolute error (MAE) between expected and modelled spectral power by each component across simulations and times. Algorithmic performance was assessed by calculating MAE in parameter estimates across simulations and times relative to expected parameters. Peak-fitting probability in the alpha (5.5-10.5 Hz) and beta (13.5-20.5 Hz) bands were calculated for each time bin as the fraction of simulations with at least one oscillatory peak recovered in the frequency band of interest.

Generic time series simulations

For each time series generation, we sampled the parameter values of their a/rhythmic components uniformly from realistic ranges. Aperiodic exponents were initialized between 0.8-2.2 Hz^{-1}. Aperiodic offsets were initialized between -8.1 and -1.5 a.u. Within the 12-36 s time segment into the simulation (onset randomized), the aperiodic exponent and offset underwent a linear shift of magnitude in the ranges -0.5 to 0.5 Hz^{-1} and -1 to 1 a.u. (sampled continuously, chosen randomly), respectively. The duration of the linear shift was randomly selected for each simulated time series between 6 and 24 s. Between 0-4 oscillatory (rhythmic) components were added to each trial with parameters randomly sampled within the following ranges: centre frequency: 3-35 Hz; amplitude: 0.6-1.6 a.u.; standard deviation: 1-2 Hz. The onset (5-40 s) and duration (3-20 s) of each of the rhythmic components were also randomized across components and across trials, with the constraint that they would not overlap both in time and frequency; they were allowed to overlap in either dimension. If a rhythmic component overlapped temporally with another one, its centre frequency was set at least 2.5 peak standard deviations from the other temporally overlapping

rhythmic component(s). The magnitude of each periodic component was tapered by a Tukey kernel (cosine fraction = 0.4).

Each simulation was analyzed with SPRiNT using 5x1s STFT windows with 50% overlap (frequency range: 1-40 Hz). Settings for *specparam* were: peak width limits: [0.5 6]; maximum number of peaks: 6; minimum peak amplitude: 0.6 a.u.; peak threshold: 2.0 standard deviations; proximity threshold: 2 standard deviations; aperiodic mode: fixed. Settings for peak post-processing were: number of neighbouring peaks: 3; centre frequency: 2.5 Hz; time bin: 6 bins (= 3 s). The spectrogram outcome of SPRiNT was analyzed to identify rhythmic components as correct (i.e., present in ground truth signal) or incorrect components. Rhythmic SPRiNT components were labelled as correct if their centre frequency was within 2.5 peak standard deviations from any of the ground truth rhythmic components. In the event of multiple SPRiNT rhythmic components meeting these conditions, we selected the one with the largest amplitude peak (marking the other as incorrect).

Errors on parameter estimates were assessed via MAE measures with respect to their ground truth values. The peak-fitting probability for each simulated rhythmic component was derived as the fraction of correct peaks recovered when one was expected. Model fit error was calculated for each time bin as the MAE between empirical and SPRiNT spectral power. We used a linear regression model (*fitlm* MATLAB function; 2020a; Natick, MA) to predict model fit errors at each time bin, using number of simulated peaks as a predictor.

$$MAE = intercept + B * number\ of\ simulated\ peaks$$

Study 2: Resting-state electrophysiology data

We used open-access resting-state electroencephalography (EEG) and demographics data collected for 212 participants from the Leipzig Study on Mind-Body-Emotion Interactions (LEMON; Babayan et al., 2019). Participants were asked to alternate every 60 seconds between eyes-open and eyes-closed resting-state for 16 minutes. Continuous EEG activity (2500-Hz sampling rate) was recorded from 61 Ag/AgCl active electrodes placed in accordance with the 10-10 system. An electrode below the right eye recorded eye-blinks (ActiCap System, Brain Products). Impedance of all electrodes was maintained below 5 kΩ. EEG recordings were referenced to FCz during data collection (Babayan et al., 2019), and re-referenced to an average reference during preprocessing.

Preprocessing was performed using *Brainstorm* (Tadel et al., 2011). Recordings were resampled to 250 Hz before being high-pass filtered at 0.1 Hz using a Kaiser window. Eyeblink EEG artifacts were detected and removed using SSP projectors. Data was visually inspected for bad channels and artifacts exceeding 200 μV. 20 participants were excluded for not following task instructions, 2 for failed recordings, 1 for data missing event markers, and 11 were excluded for EEG data of poor quality (> 8 bad sensors). The results herein are from the remaining 178 participants (average number of bad sensors = 3). We extracted the first 5 minutes of consecutive quality data, beginning with the eyes-closed condition, from electrode Oz for each participant.

Spectrogram analysis

Each recording block was analyzed with SPRiNT using 5x1s sliding time windows with 50% overlap (frequency range: 1-40 Hz). We ran SPRiNT using the Brainstorm implementation with the following settings: peak width limits: [1.5 6]; maximum number of peaks: 3; minimum peak

amplitude: 0.5 a.u.; peak threshold: 2.0 standard deviations; proximity threshold: 2.5 standard deviations; aperiodic mode: fixed. Peak post-processing was run on SPRiNT outputs (number of neighbouring peaks 3; centre frequency: 2.5 Hz; time bin: 6 bins (= 3 s). Alpha peaks were defined as all oscillatory peaks parameterized between 6-14 Hz. To capture variability in alpha peak centre frequency across time, mean and standard deviations of alpha peak centre frequency distributions were computed across both eyes -open and -closed conditions and by age group (defined below).

We also computed spectrograms from Morlet wavelet time-frequency decompositions (1-40 Hz, in 1 Hz steps) also using Brainstorm (with default parameters; central frequency = 1 Hz, FWHM = 3 s; Tadel et al., 2011).

Contrast between eyes-open and eyes-closed conditions

All regression analyses were performed in R (V 3.6.3; R Core Team, 2020). We ran a logistic regression model whereby we predicted the condition (i.e., eyes-open vs eyes-closed) from the mean and standard deviation of the following SPRiNT parameters: alpha centre frequency, alpha power, and aperiodic exponent. All model predictors were entered as fixed effects. Significance of each beta coefficient was tested against zero (i.e., $B_n = 0$). We quantified the evidence for each predictor in our models with a Bayes factor analysis where we systematically removed one of the predictors and computed the Bayes factor using the *BayesFactor* library (Morey & Rouder, 2018). We compared the most complex model (i.e., the full model) against all models formulated by removing a single predictor. Evidence in favor of the full model (i.e., BF < 1) indicated that a given predictor improved model fit, whereas evidence for the model without the predictor (i.e., BF > 1) showed limited improvement in terms of model fit.

We also fitted a logistic regression model to predict experimental condition (i.e., eyes -open & -closed; dummy coded) from mean alpha-band power (6-14 Hz) entered as a fixed effect. Alpha-band power was computed as the mean log-power between 6-14 Hz for each condition extracted from the Morlet wavelets spectrograms. Significance of each beta coefficient was tested against zero (i.e., $B_n = 0$).

Predicting age from resting-state activity

Participants were assigned to two groups based on their biological age: younger adults (age: 20-40 years, $n = 121$) and older adults (age: 55-80 years, $n = 57$). Modelled alpha peaks and aperiodic parameters were collapsed across time to generate condition-specific distributions of model parameters per participant. We used these distributions to examine the mean and standard deviation of alpha centre frequency, alpha power, and aperiodic exponent. We fitted two logistic regression models using the *glm* function in R (R Core Team, 2020) for the eyes-open and eyes-closed conditions:

All predictors were entered as fixed effects. Significance of each beta coefficient was tested against zero (i.e., $B_n = 0$). We also quantified the evidence for each predictor in our models with a Bayes factor analysis.

Study 3: Intracranial rodent data

Local field potential (LFP) recordings and animal behaviour, originally published by Mizuseki et al. (2009), were collected from 2 Long-Evans rats (data retrieved from https://crcns.org). Animals were implanted with eight-shank multi-site silicon probes (200 µm inter-shank distance) spanning multiple layers of dorsocaudal medial entorhinal cortex (entorhinal cortex, dentate gyrus,

583 hippocampus). Neurophysiological signals were recorded while animals traversed to alternating
584 ends of an elevated linear track (250 x 7 cm) for 30 µL water reward (animals were water deprived
585 for 24 hrs prior to task). Recordings were acquired continuously at 20 kHz (RC Electronics) and
586 bandpass-filtered (1 Hz-5 kHz) before being down-sampled to 1250 Hz. In two rats (EC012,
587 EC013), nine recording blocks of activity in entorhinal cortex layer 3 (EC3) were selected for
588 further analysis (16 electrodes in EC012, 8 electrodes in EC013). Data from one electrode in
589 EC012 was removed for having poor quality. Animal head position was extracted from video
590 recordings (39.06 Hz) of two head-mounted LEDs and temporally interpolated to align with
591 SPRiNT parameters across time (piecewise cubic Hermite interpolative polynomial; pchip in
592 MATLAB; 2020a; Natick, MA).
593
594 ***Spectrogram analysis***
595 Each recording block was analyzed with SPRiNT using 5x2 s sliding time windows with 75%
596 overlap (frequency range: 2-40 Hz). Settings for specparam were set as: peak width limits: [1.5 5];
597 maximum number of peaks: 3; minimum peak amplitude: 0.5 a.u.; peak threshold: 2.0 standard
598 deviations; proximity threshold: 2.0 standard deviations; aperiodic mode: fixed. Settings for peak
599 post-processing were set as: number of neighbouring peaks: 3; centre frequency bounds: 2.5 Hz;
600 time bin bounds: 6 bins (= 3 s). Aperiodic parameters were averaged across electrodes and aligned
601 with behavioural data.
602
603 ***Tracking aperiodic dynamics during movement transitions***
604 Time bins were categorized based on whether animals were resting at either end of the track or
605 moving toward opposite ends of the track (‘rest’ or ‘movement’, respectively) using animal

position (and speed). Rest-to-movement and movement-to-rest transitions were defined as at least four consecutive seconds of rest followed by four consecutive seconds of run (t = 0 representing the onset of movement), or vice-versa (t = 0 representing the onset of rest), respectively.

Software and code availability

The SPRiNT algorithm and all code needed to produce the figures shown are available from GitHub (https://github.com/lucwilson/SPRiNT). The SPRiNT algorithm is also available from the Brainstorm distribution (Tadel et al., 2011).

Data availability

The simulated data are openly available on OSF (https://osf.io/c3gn4/). Resting-state EEG data was obtained from the open repository LEMON (Babayan et al., 2019; https://openneuro.org/datasets/ds000221/versions/00002). Intracranial rodent data (study HC3) is openly available from Mizuseki et al. (2009; data retrieved from https://crcns.org). SPRiNT-processed data is available upon request from the corresponding author.

Author contributions

All authors conceptualized the study, L.E.W. and J.D.S.C. preformed the analyses, S.B. provided guidance with data interpretation, all authors contributed to the writing and editing of the manuscript.

Competing interests

The authors declare no competing financial interest.

Acknowledgements

L.E.W. acknowledges the support of an NSERC Undergraduate Student Research Award. J.D.S.C. acknowledges the support of the Alexander Graham-Bell Doctoral NSERC fellowship. S.B. is grateful for the support received from the NIH (R01 EB026299), a Discovery Grant from the Natural Science and Engineering Research Council of Canada (436355-13), the CIHR Canada Research Chair in Neural Dynamics of Brain Systems, the Brain Canada Foundation with support from Health Canada, and the Innovative Ideas program from the Canada First Research Excellence Fund, awarded to McGill University for the Healthy Brains for Healthy Lives initiative. This research was undertaken thanks in part to funding from the Canada First Research Excellence Fund, awarded to McGill University for the Healthy Brains for Healthy Lives initiative.

651 **Figures**

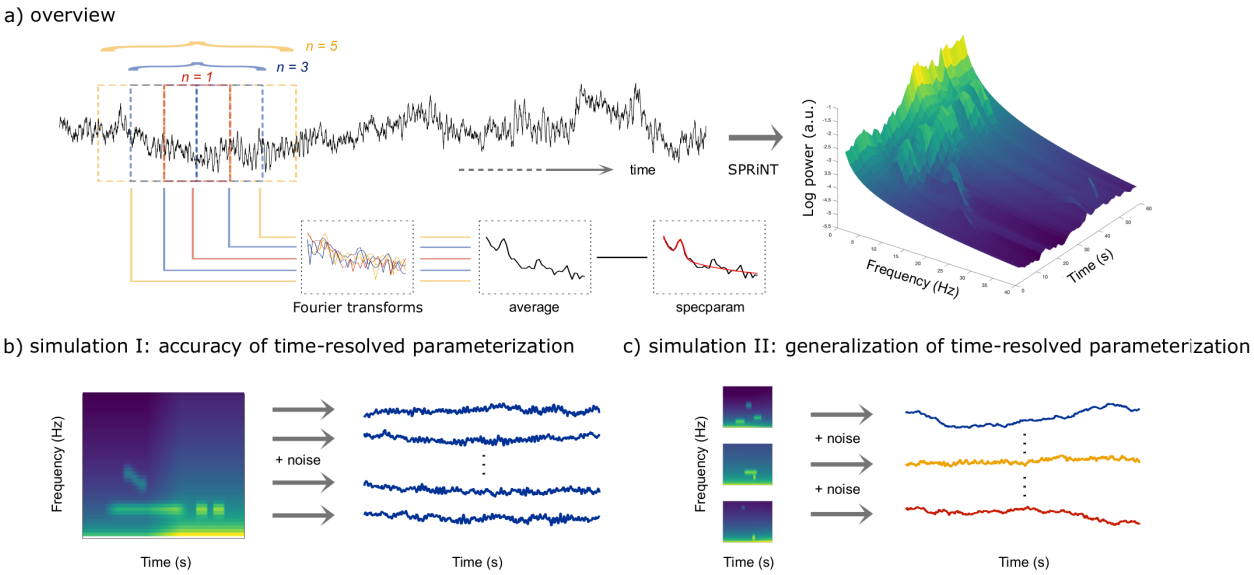

652

653 ***Figure 1: Methods Synopsis***

654 (**A**) Overview of the approach implemented in SPRiNT. At each time bin along a neural time
655 series (black trace) *n* overlapping time windows are Fourier-transformed to yield an estimate of
656 spectral contents, which is subsequently parameterized using *specparam* (Donoghue et al.,
657 2020). The procedure is replicated across time over sliding windows to generate a parameterized
658 spectrogram of neural activity. (**B**) Simulation challenge I. We simulated 10,000 time-series
659 composed of time-varying spectral (aperiodic and periodic) features. These ground-truth time
660 series were used to evaluate the respective performances of SPRiNT and those from a wavelet-
661 *specparam* alternative. (**C**) Simulation challenge II. We simulated another 10,000 time series
662 each composed of different time-varying spectral (aperiodic and periodic) ground-truth features.
663 These time series were used to assess SPRiNT's ability to detect these features.

664

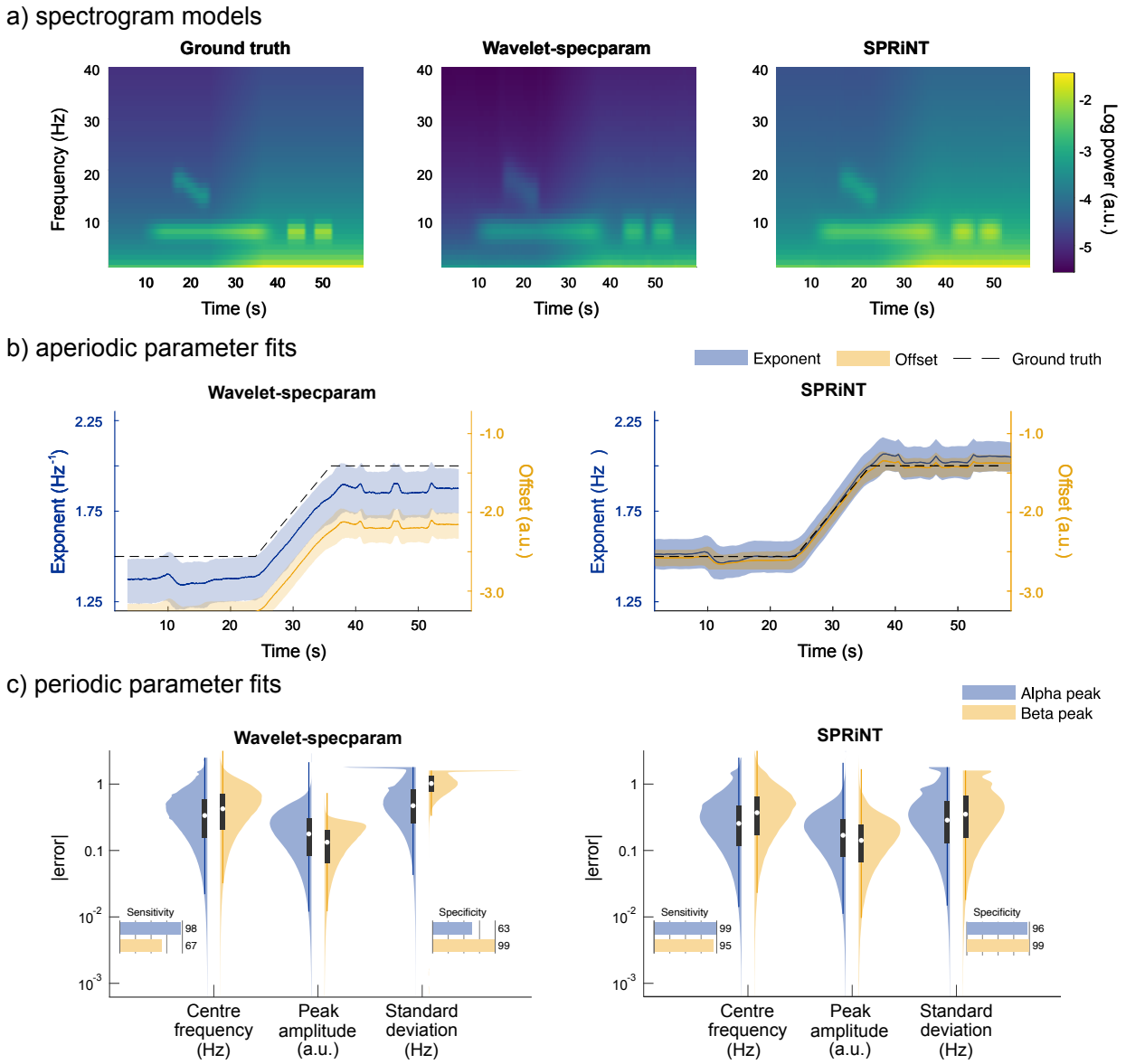

Figure 2: SPRiNT vs. wavelet-specparam performances (Simulation Challenge I).

(A) Ground truth spectrogram (left) and averaged modelled spectrograms from the wavelet-*specparam approach* (middle) and SPRiNT (right; n = 10,000). (**B**) Aperiodic parameter estimates (lines: median; shaded regions: first and third quartiles, n = 10,000) across time from wavelet-specparam (left) and SPRiNT (right; black: ground truth; blue: exponent; yellow: offset). (**C**) Absolute error (and detection performance) of alpha and beta-band rhythmic components for wavelet-*specparam* (left) and SPRiNT (right). Violin plots represent the sample

distributions (*n* =10,000; blue: alpha peak; yellow: beta peak; white circle: median, grey box: first and third quartiles; whiskers: range).

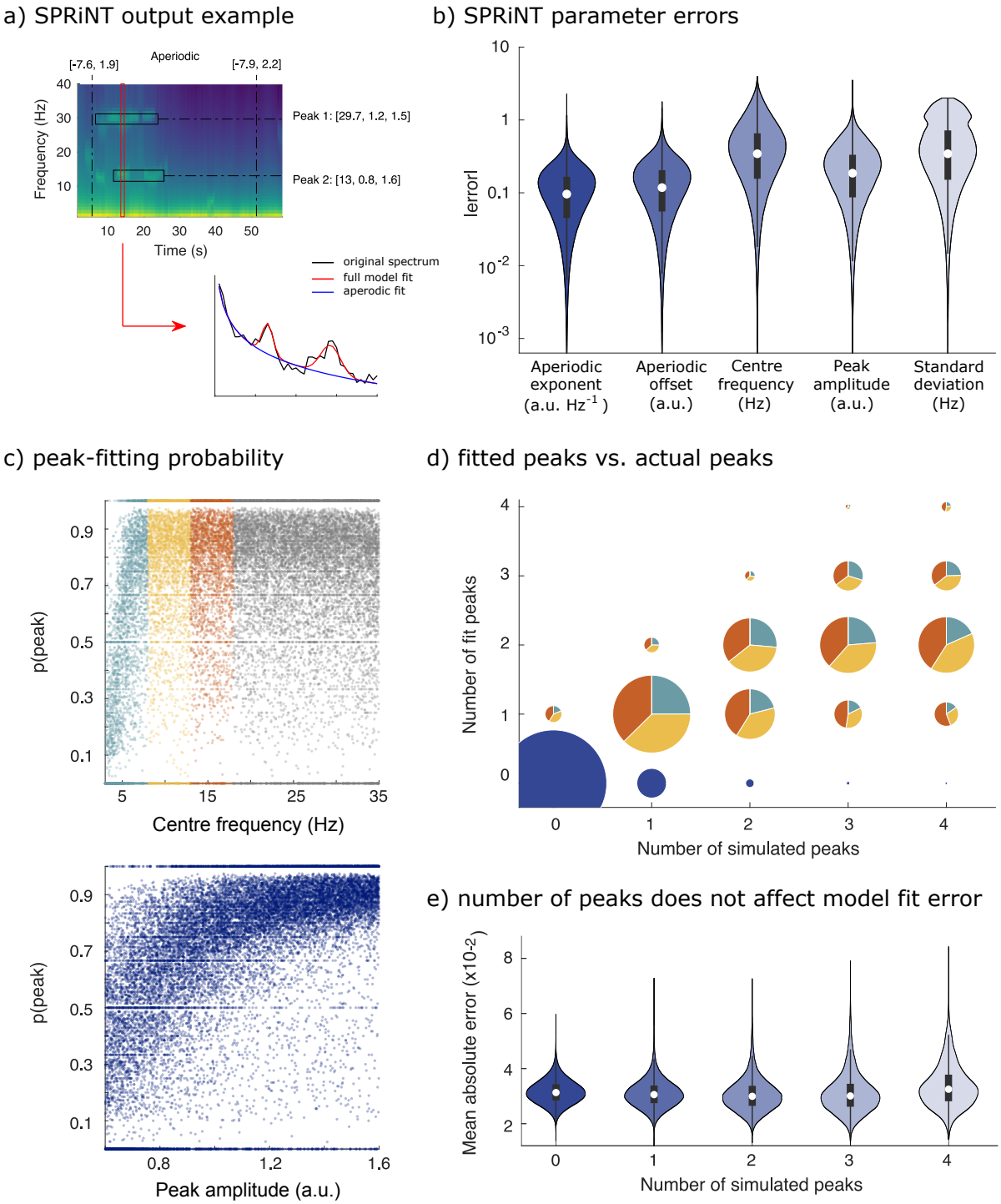

Figure 3: SPRiNT raw performance (Simulation Challenge II).

(A) SPRiNT parameterized spectrogram for a representative simulated time series with time-varying aperiodic (offset, exponent) and transient periodic (centre frequency, amplitude, standard deviation) components. The red arrow indicates a cross-sectional view of the spectrogram at 14 s. (**B**) Absolute error in SPRiNT parameter estimates across all simulations (*n* =10,000). (**C**) Detection probability of spectral peaks (i.e., rhythmic components) depending on simulated centre frequency and amplitude (light blue: 3-8 Hz theta; yellow: 8-13 Hz alpha; orange: 13-18 Hz beta). (**D**) Number of fitted vs. simulated rhythmic components (spectral peaks), across all simulations and time points. The underestimation of the number of estimated spectral peaks is related to centre frequency: 3-8 Hz simulated peaks (blue) account for proportionally fewer of recovered peaks between 3-18 Hz (blue, yellow, orange) than from the other two tertiles. (Samples sizes by number of simulated peaks: 0 peaks = 798,753, 1 peak = 256,599, 2 peaks = 78,698, 3 peaks =14,790, 4 peaks = 1,160) (E) Model fit error is not affected by number of simulated peaks. Violin plots show the full sample distributions (white circle: median, grey box: first and third quartiles; whiskers: range).

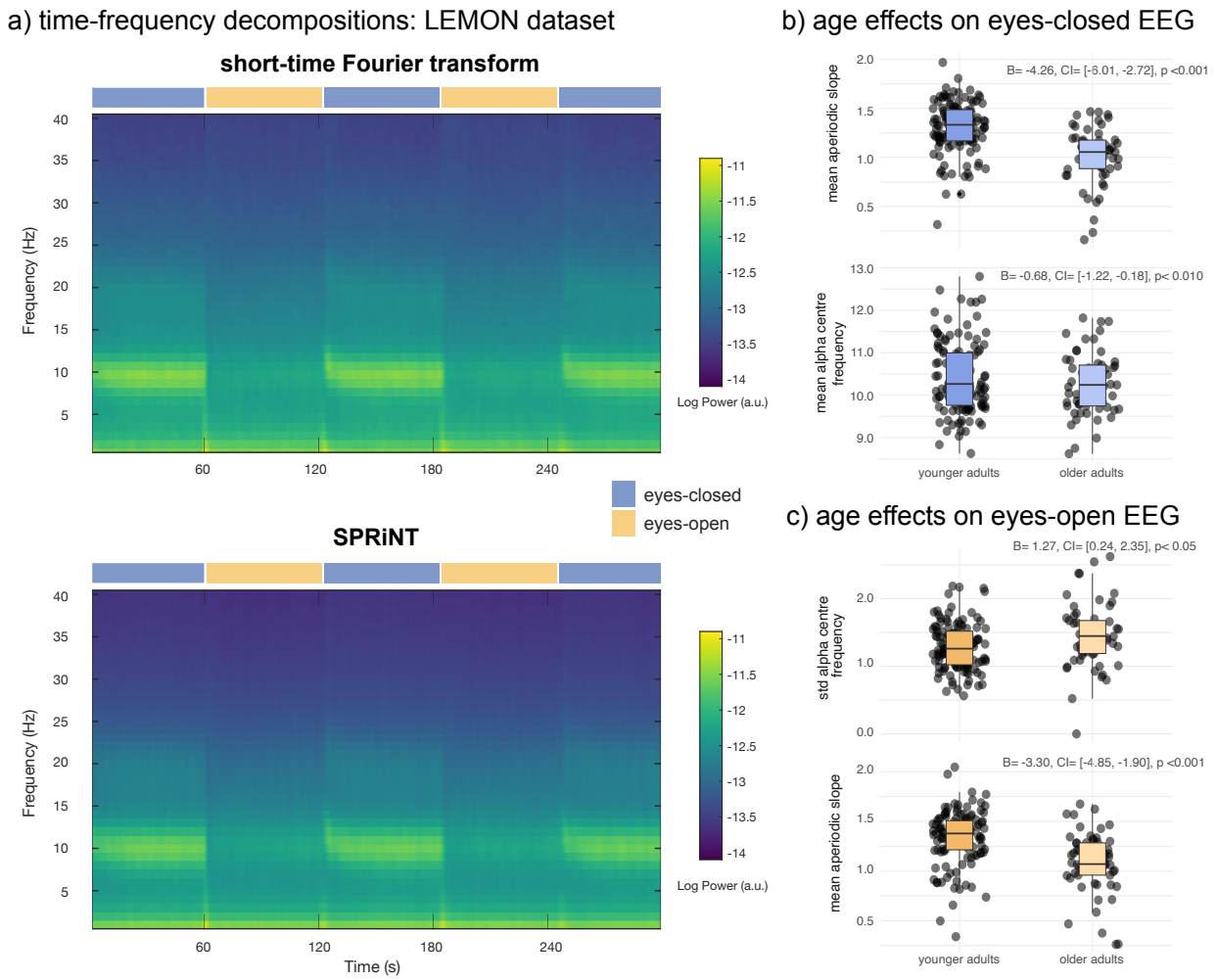

Figure 4: SPRiNT parameterization of resting-state electroencephalography

(A) We generated spectrograms across all participants (n = 178) over 5 min of continuous eyes-closed-eyes-open recordings from electrode Oz, using both short-time Fourier transforms (top) and SPRiNT (bottom). **(B)** Logistic regression models indicated that mean aperiodic exponent and mean alpha centre frequency parameters in eyes-closed resting-state data are predictive of age group. **(C)** Logistic regression models indicated that mean aperiodic exponent and variability (standard deviation) of alpha centre frequency parameters in eyes-closed resting-state data are predictive of age group (boxplot line: median; boxplot limits: first and third quartiles; whiskers: range). Sample sizes: younger adults (age: 20-40 years): 121; older adults (age: 55-80 years): 57.

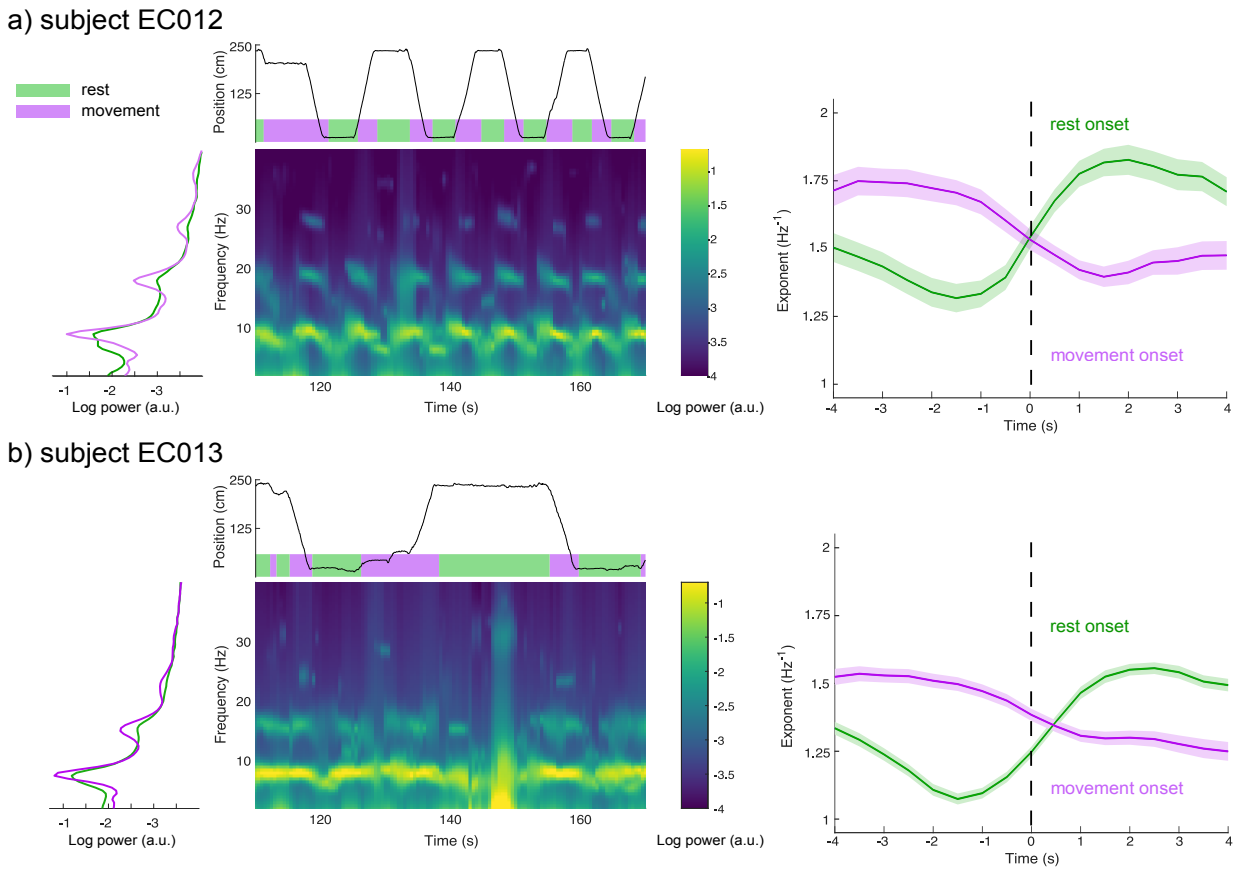

Figure 5: SPRiNT captures aperiodic dynamics related to locomotion

(A) We generated power spectra collapsed across rest (green) and movement (purple) periods for subject EC012, observing broad increases in spectral power in frequencies below 20 Hz during rest relative to movement. A sample SPRiNT model spectrogram is provided, with position time series located above (green: rest; purple: movement). We observed gradual shifts around locomotor transitions of aperiodic exponent (right), with increasing exponents at the onset of rest and decreasing exponents at movement onset (solid line: mean; shaded region: 95% CI). **(B)** Same data as (A), but for subject EC013. Sample sizes: EC012 rest onset (green): 67 epochs; EC012 movement onset (purple): 89 epochs; EC013 rest onset: 323 epochs; EC013 movement onset: 263 epochs.

References

Albouy, P., Weiss, A., Baillet, S., & Zatorre, R. J. (2017). Selective Entrainment of Theta Oscillations in the Dorsal Stream Causally Enhances Auditory Working Memory Performance. *Neuron*, *94*(1), 193-206.e195. doi:10.1016/j.neuron.2017.03.015

Alhourani, A., Wozny, T. A., Krishnaswamy, D., Pathak, S., Walls, S. A., Ghuman, A. S., . . . Niranjan, A. (2016). Magnetoencephalography-based identification of functional connectivity network disruption following mild traumatic brain injury. *J Neurophysiol, 116*(4), 1840-1847. doi:10.1152/jn.00513.2016

Babayan, A., Erbey, M., Kumral, D., Reinelt, J. D., Reiter, A. M. F., Röbbig, J., . . . Villringer, A. (2019). A mind-brain-body dataset of MRI, EEG, cognition, emotion, and peripheral physiology in young and old adults. *Scientific Data*, *6*(1), 180308. doi:10.1038/sdata.2018.308

Bruns, A. (2004). Fourier-, Hilbert- and wavelet-based signal analysis: are they really different approaches? *Journal of Neuroscience Methods, 137*(2), 321-332. doi:10.1016/j.jneumeth.2004.03.002

Buzsáki, G. (2006). *Rhythms of the brain*. Oxford: Oxford University Press.

Buzsáki, G., & Watson, B. O. (2012). Brain rhythms and neural syntax: implications for efficient coding of cognitive content and neuropsychiatric disease. *Dialogues in clinical neuroscience*, *14*(4), 345-367. doi: 10.31887/DCNS.2012.14.4/gbuzsaki

Cellier, D., Riddle, J., Petersen, I., & Hwang, K. (2021). The development of theta and alpha neural oscillations from ages 3 to 24 years. *Developmental Cognitive Neuroscience*, *50*, 100969. doi:10.1016/j.dcn.2021.100969

Chini, M., Pfeffer, T., & Hanganu-Opatz, I. L. (2021). Developmental increase of inhibition drives decorrelation of neural activity. *bioRxiv*, 2021.2007.2006.451299. doi:10.1101/2021.07.06.451299

Cohen, M. X. (2014). *Analyzing neural time series data: Theory and practice*. Boston: MIT Press.

Cole, S., Donoghue, T., Gao, R., & Voytek, B. (2019). NeuroDSP: A package for neural digital signal processing. *Journal of Open Source Software, 4*(36), 1272. doi:10.21105/joss.01272

da Silva Castanheira, J., Orozco Perez, H. D., Misic, B., & Baillet, S. (2021). Brief segments of neurophysiological activity enable individual differentiation. *Nature Communications*, *12*(1), 5713. doi:10.1038/s41467-021-25895-8

Donoghue, T., Haller, M., Peterson, E. J., Varma, P., Sebastian, P., Gao, R., . . . Knight, R. T. (2020). Parameterizing neural power spectra into periodic and aperiodic components. *Nature Neuroscience, 23*(12), 1655-1665. doi:10.1038/s41593-020-00744-x

Donoghue, T., Schaworonkow, N., & Voytek, B. (2021). Methodological considerations for studying neural oscillations. *Eur J Neurosci*. doi:10.1111/ejn.15361

Gao, R., Peterson, E. J., & Voytek, B. (2017). Inferring synaptic excitation/inhibition balance from field potentials. *NeuroImage, 158*, 70-78. doi:10.1016/j.neuroimage.2017.06.078

Haegens, S., Cousijn, H., Wallis, G., Harrison, P. J., & Nobre, A. C. (2014). Inter- and intra-individual variability in alpha peak frequency. *NeuroImage, 92*, 46-55. doi:10.1016/j.neuroimage.2014.01.049

He, B. J. (2014). Scale-free brain activity: Past, present, and future. *Trends in Cognitive Sciences, 18*(9), 480-487. doi:10.1016/j.tics.2014.04.003

Kucewicz, M. T., Cimbalnik, J., Matsumoto, J. Y., Brinkmann, B. H., Bower, M. R., Vasoli, V., . . . Worrell, G. A. (2014). High frequency oscillations are associated with cognitive processing in human recognition memory. *Brain, 137*(8), 2231-2244. doi:10.1093/brain/awu149

Larsson, P. G., & Kostov, H. (2005). Lower frequency variability in the alpha activity in EEG among patients with epilepsy. *Clinical Neurophysiology, 116*(11), 2701-2706. doi:10.1016/j.clinph.2005.07.019

Mizuseki, K., Sirota, A., Pastalkova, E., & Buzsáki, G. (2009). Theta Oscillations Provide Temporal Windows for Local Circuit Computation in the Entorhinal-Hippocampal Loop. *Neuron*, *64*(2), 267-280. doi:10.1016/j.neuron.2009.08.037

Moca, V. V., Bârzan, H., Nagy-Dăbâcan, A., & Mureșan, R. C. (2021). Time-frequency super-resolution with superlets. *Nature Communications, 12*(1), 337. doi:10.1038/s41467-020-20539-9

Molina, J. L., Voytek, B., Thomas, M. L., Joshi, Y. B., Bhakta, S. G., Talledo, J. A., . . . Light, G. A. (2020). Memantine Effects on Electroencephalographic Measures of Putative Excitatory/Inhibitory Balance in Schizophrenia. *Biol Psychiatry Cogn Neurosci Neuroimaging, 5*(6), 562-568. doi:10.1016/j.bpsc.2020.02.004

Morey, R. D., & Rouder, J. N. (2018). BayesFactor: Computation of Bayes factors for common designs. R package version 0.9.12-4.2. Retrieved from https://CRAN.R-project.org/package=BayesFactor

Ostlund, B. D., Alperin, B. R., Drew, T., & Karalunas, S. L. (2021). Behavioral and cognitive correlates of the aperiodic (1/f-like) exponent of the EEG power spectrum in adolescents with and without ADHD. *Developmental Cognitive Neuroscience, 48*, 100931. doi:10.1016/j.dcn.2021.100931

Ostlund, B., Donoghue, T., Anaya, B., Gunther, K. E., Karalunas, S. L., Voytek, B., & Pérez-Edgar, K. E. (2022). Spectral parameterization for studying neurodevelopment: How and why. Developmental Cognitive Neuroscience, 54, 101073. doi:/10.1016/j.dcn.2022.101073

Ouyang, G., Hildebrandt, A., Schmitz, F., & Herrmann, C. S. (2020). Decomposing alpha and 1/f brain activities reveals their differential associations with cognitive processing speed. *NeuroImage*, *205*, 116304. doi:10.1016/j.neuroimage.2019.116304

Pathania, A., Schreiber, M., Miller, M. W., Euler, M. J., & Lohse, K. R. (2021). Exploring the reliability and sensitivity of the EEG power spectrum as a biomarker. *International Journal of Psychophysiology, 160*, 18-27. doi:10.1016/j.ijpsycho.2020.12.002

Pietrelli, M., Samaha, J., & Postle, B. R. (2021). Spectral distribution dynamics across different attentional priority states. *bioRxiv*, 2021.2012.2002.470964. doi:10.1101/2021.12.02.470964

R Core Team. (2020). *R: A language and environment for statistical computing*. R Foundation for Statistical Computing, Vienna, Austria. Retrieved from https://www.R-project.org/

Samaha, J., Iemi, L., Haegens, S., & Busch, N. A. (2020). Spontaneous Brain Oscillations and Perceptual Decision-Making. *Trends in Cognitive Sciences*, *24*(8), 639-653. doi:10.1016/j.tics.2020.05.004

Samiee, S., & Baillet, S. (2017). Time-resolved phase-amplitude coupling in neural oscillations. *NeuroImage*, *159*, 270-279. doi:10.1016/j.neuroimage.2017.07.051

Scally, B., Burke, M. R., Bunce, D., & Delvenne, J.-F. (2018). Resting-state EEG power and connectivity are associated with alpha peak frequency slowing in healthy aging. *Neurobiology of Aging*, *71*, 149-155. doi:10.1016/j.neurobiolaging.2018.07.004

Schaworonkow, N., & Voytek, B. (2021). Longitudinal changes in aperiodic and periodic activity in electrophysiological recordings in the first seven months of life. *Developmental Cognitive Neuroscience, 47*, 100895. doi:10.1016/j.dcn.2020.100895

Schwarz, G. (1978). Estimating the Dimension of a Model. *The Annals of Statistics*, *6*(2), 461-464. doi:10.1214/aos/1176344136

Studenova, A. A., Villringer, A., & Nikulin, V. V. (2021). Baseline shift in neuronal oscillations and its implications for the interpretation of evoked activity obtained with EEG/MEG. *bioRxiv*, 2021.2012.2001.470793. doi:10.1101/2021.12.01.470793

Tadel, F., Baillet, S., Mosher, J. C., Pantazis, D., & Leahy, R. M. (2011). Brainstorm: A User-Friendly Application for MEG/EEG Analysis. *Computational Intelligence and Neuroscience, 2011*, 879716. doi:10.1155/2011/879716

van Heumen, S., Moreau, J. T., Simard-Tremblay, E., Albrecht, S., Dudley, R. W., & Baillet, S. (2021). Case Report: Aperiodic Fluctuations of Neural Activity in the Ictal MEG of a Child With Drug-Resistant Fronto-Temporal Epilepsy. *Frontiers in Human Neuroscience, 15*(101). doi:10.3389/fnhum.2021.646426

Voytek, B., & Knight, R. T. (2015). Dynamic Network Communication as a Unifying Neural Basis for Cognition, Development, Aging, and Disease. *Biological Psychiatry*, *77*(12), 1089-1097. doi:10.1016/j.biopsych.2015.04.016

Voytek, B., Kramer, M. A., Case, J., Lepage, K. Q., Tempesta, Z. R., Knight, R. T., & Gazzaley, A. (2015). Age-Related Changes in 1/*f* Neural Electrophysiological Noise. *The Journal of Neuroscience, 35*(38), 13257. doi:10.1523/JNEUROSCI.2332-14.2015

Waschke, L., Donoghue, T., Fiedler, L., Smith, S., Garrett, D. D., Voytek, B., & Obleser, J. (2021). Modality-specific tracking of attention and sensory statistics in the human electrophysiological spectral exponent. *eLife, 10*, e70068. doi:10.7554/eLife.70068

Wen, H., & Liu, Z. (2016). Separating fractal and oscillatory components in the power spectrum of neurophysiological signal. *Brain Topography, 29*(1), 13-26. doi:10.1007/s10548-015-0448-0

Supplemental Material

Detection and removal of spectrogram outlier components

A known issue of *specparam* is the fitting of spurious, outlier spectral peaks (Donoghue et al., 2020). In SPRiNT, these peaks often appear as transient blips of periodic activity in the spectrogram (Supplemental Figure S1A). We propose a post-processing option in SPRiNT to detect and remove transient periodic activity (Supplemental Figure S1B). In short, the procedure searches for clusters of spectral peaks over a user-defined maximum time period (see Methods). Once an outlier peak is detected at a given time bin and removed from the model, aperiodic parameters are refit with *specparam* to account for the variance previously attributed to the spurious peak and models are subsequently updated to reflect changes in parameters.

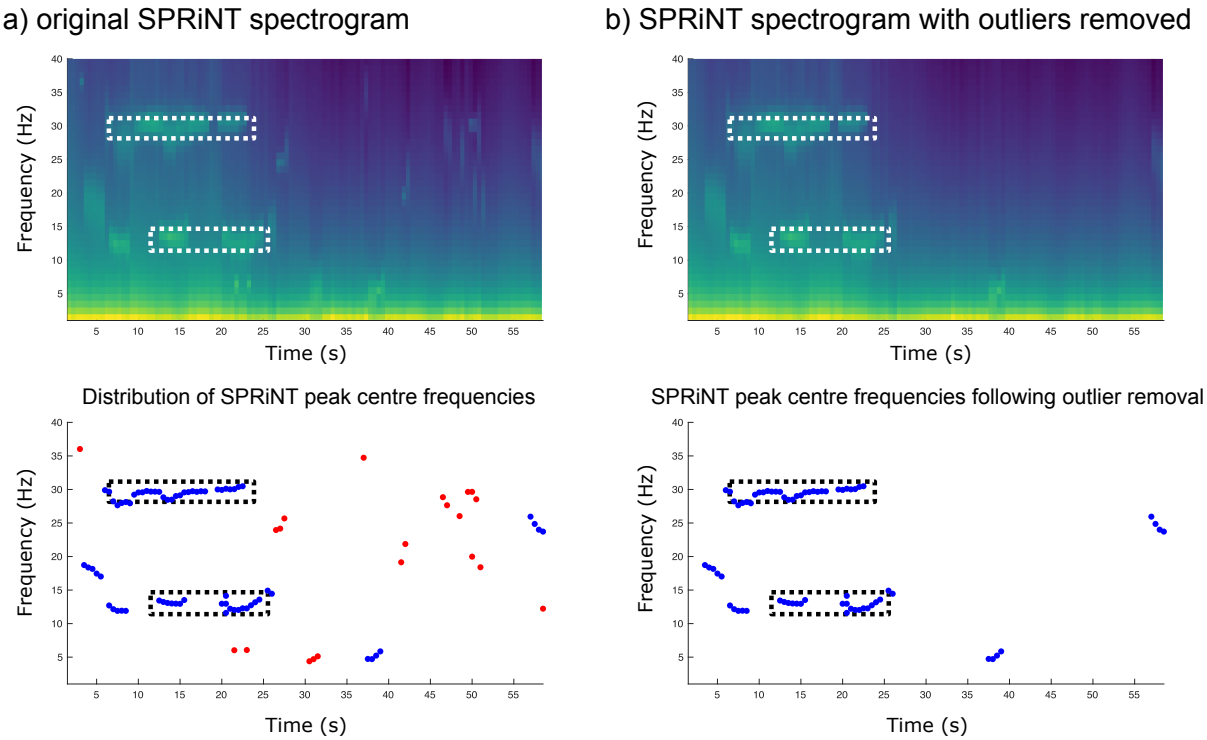

Figure S1. Overview of the outlier peak removal process.

(A) Original SPRiNT spectrogram (top) and time-frequency distribution of peak centre frequencies (bottom). In this example, the detected peaks (red and blue dots) are sequentially removed if they are not part of a cluster of contiguous peaks within a time-frequency region of 3 s and 2.5 Hz (red dots; size of minimum cluster is adjustable by user). **(B)** Resulting SPRiNT spectrogram (top) and peak centre frequencies (bottom) after outlier removal and the update of aperiodic parameters. Dashed rectangular areas show time-frequency regions where rhythmic activity was simulated in the synthesized signal.

Methods benchmarking (synthetic data Challenge I)

Below we present the results of SPRiNT from synthetic data Challenge I without outlier peak removal. We show, similar to the results presented in the main text, that SPRiNT modelled aperiodic and periodic spectrograms with low error (aperiodic model mean absolute error [MAE] = 0.07; peak model MAE = 0.04). For the aperiodic component, the algorithm accurately recovered both ground truth exponent (MAE = 0.11) and offset (MAE = 0.15). It also detected the occurrences of alpha peaks with high sensitivity (99% at time bins with maximum peak amplitude) and specificity (6% spurious detections), and with low errors on their centre frequency (MAE = 0.36) and amplitude (MAE = 0.21) parameters, but overestimated the width of the periodic peak components (MAE = 0.42). The algorithm detected and tracked the down-chirping beta periodic components with high sensitivity (95% at time bins with maximum peak amplitude) but lower specificity (95%) than with outlier peak removal (99%). Time-collapsed errors on centre frequency (MAE = 0.48) and amplitude (MAE = 0.18) parameters were low, with a tendency to overestimate the width in frequency of the periodic component (MAE = 0.48). Results following outlier peak removal are presented and discussed in the main text.

We also parameterized power spectral densities of each simulation using *specparam* to assess how the results the first simulation challenge would appear if we assumed stationary spectral content across time. The PSD was computed using 1 s windows with 50% overlap. Settings for *specparam* were set as: frequency range: 1-40 Hz, in 1 Hz steps; peak width limits: [1.5 6]; maximum number of peaks: 3; minimum peak amplitude: 0.6 a.u.; peak threshold: 2.0 standard deviations; proximity threshold: 2.0 standard deviations; aperiodic mode: fixed.

The average recovered aperiodic exponent was 1.94 Hz^{-1} (actual = 1.5 to 2 Hz^{-1}) and offset was -1.64 a.u. (actual = -2.56 to -1.41 a.u.). The only peak recovered (99% sensitivity) was the alpha peak, with an average center frequency of 8.09 Hz (actual = 8 Hz), amplitude of 0.79 a.u. (actual max = 1.2 Hz), and standard deviation of 1.21 Hz (actual = 1.2 Hz); no beta peak was detected across all spectra.

Wavelet-*specparam* without temporal smoothing (synthetic data Challenge I)

We parameterized Morlet wavelet spectrograms (central frequency = 1 Hz, FWHM = 3 s; 1-40 Hz, in 1 Hz steps) of the first 1,000 simulated time series consisting of transient alpha and down-chirping beta periodic activity (time range: 1.5-58.5 s, in 0.005 s steps). Settings for *specparam* were: peak width limits: [0.5 6]; maximum number of peaks: 3; minimum peak amplitude: 0.6 a.u.; peak threshold: 2.0 standard deviations; proximity threshold: 2.0 standard deviations; aperiodic mode: fixed. In the main text, we discuss results from temporally smoothed wavelet spectrograms (see Methods). Here, we show results without temporal smoothing.

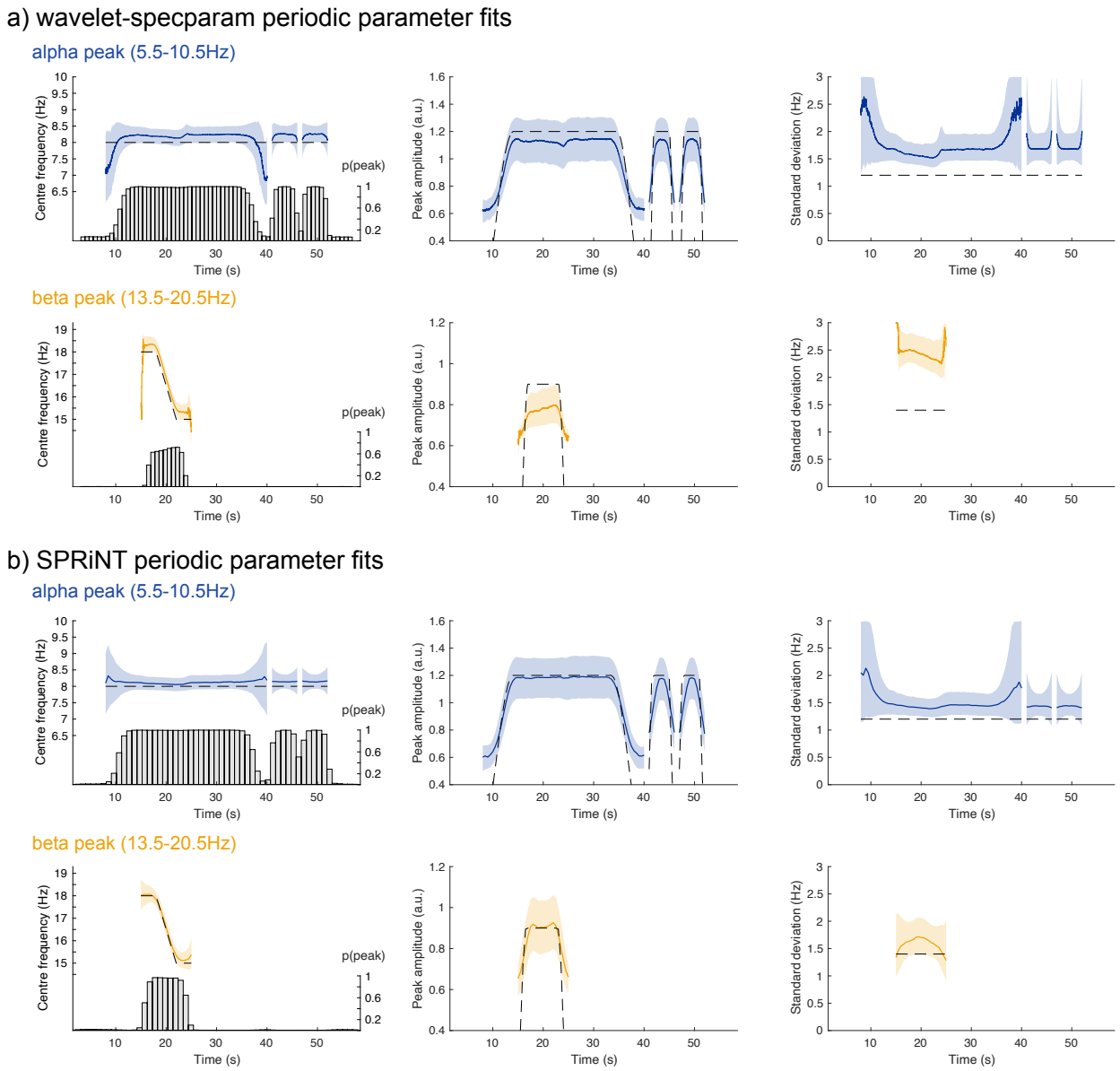

Figure S2. Periodic parameter estimates across time (*n* = 10,000 simulations). (A) Results from the temporally smoothed *wavelet-specparam approach* for the alpha (top) and beta (bottom) rhythmic components For each estimated parameter (from left to right: centre frequency, spectral peak amplitude and standard deviation), the grey dashed line indicates ground truth values over time, the plain colored line shows the median of estimates and the shaded region

their first and third quartiles. The bar plots in the left panel indicate the sample probability (over 10,000 simulations) of a detection of spectral peak at each time bin.

(B) Same display for the results obtained with SPRiNT.

Error in estimates from unsmoothed parameterized wavelet spectrograms of exponent (MAE = 0.43) and offset (MAE = 0.82) parameters were worse than those obtained from smoothed wavelet decompositions (exponent MAE = 0.19; offset MAE = 0.79). Alpha peaks were recovered with lower sensitivity (74% at time bins with maximum peak amplitude) and specificity (32% spurious detections), and with greater errors on centre frequency (MAE = 0.86), amplitude (MAE = 0.58), and bandwidth (MAE = 0.90). The down-chirping beta oscillation was detected with lower sensitivity (46% at time bins with maximum peak amplitude) and specificity (83%), and with greater errors on centre frequency (MAE = 1.31), amplitude (MAE = 0.66), and bandwidth (MAE = 1.09).

Generalization of SPRiNT across generic aperiodic and periodic fluctuations without outlier removal (synthetic data Challenge II)

We present the results of the second synthetic data challenge without outlier peak removal (Supplemental Figure S3). SPRiNT recovered 72% of the simulated periodic components, with 67% specificity (Supplemental Figure S4). Dynamic aperiodic exponents were recovered with a MAE of 0.13, while dynamic offsets were recovered with a MAE of 0.16 (Supplemental Figure S3B). Centre frequency, amplitude, and standard deviation parameters were recovered with MAEs of 0.49, 0.24, and 0.51, respectively (Supplemental Figure S3B).

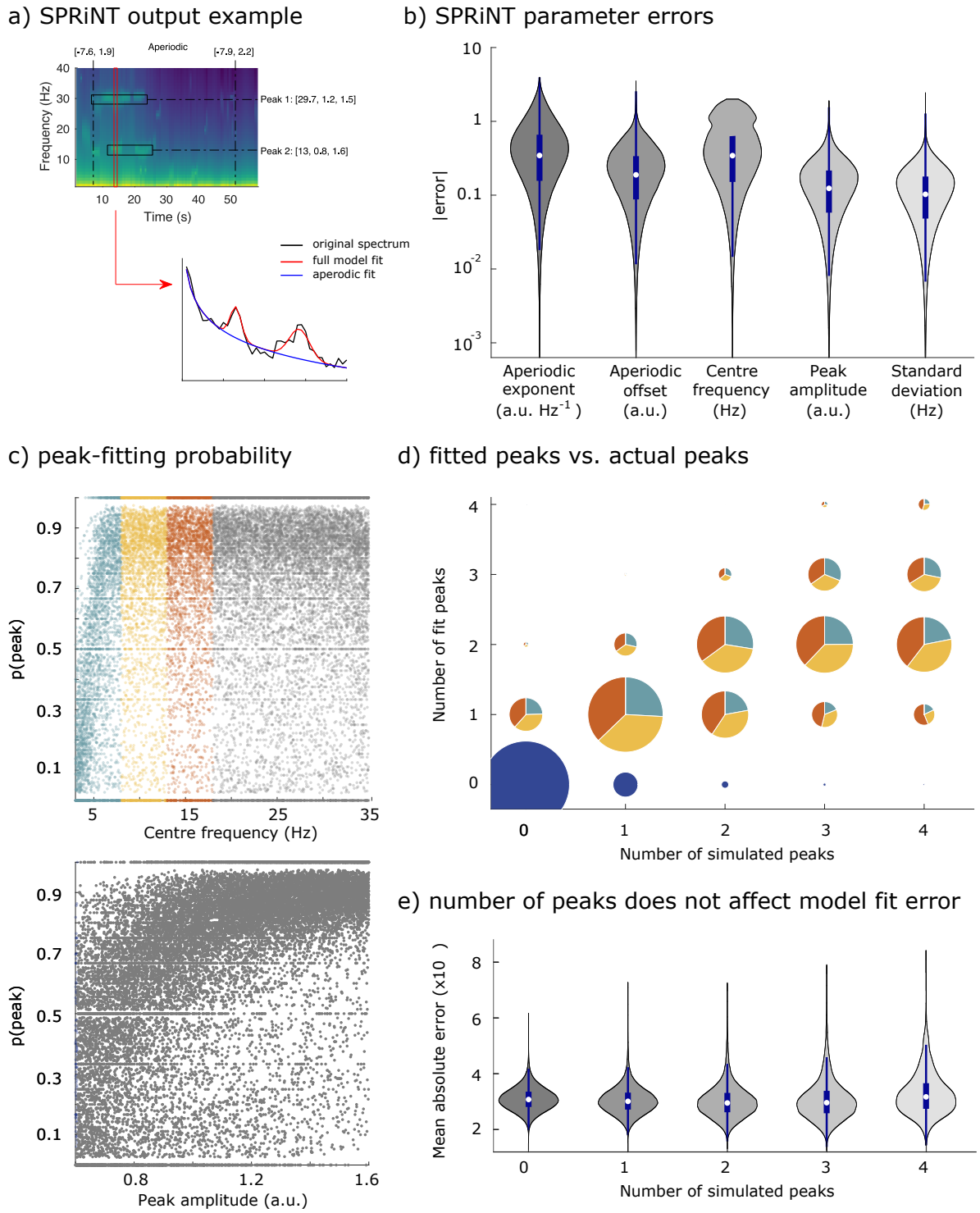

Figure S3. SPRiNT raw performance (without outlier peak removal).

(A) SPRiNT parameterized spectrogram for a representative simulated time series with time-varying aperiodic (offset, exponent) and transient periodic (centre frequency, amplitude, standard

deviation) components. The red arrow indicates a cross-sectional view of the spectrogram at 14 s. **(B)** Absolute error in SPRiNT parameter estimates across all simulations (*n* =10,000). (C) Detection probability of spectral peaks (i.e., rhythmic components) depending on simulated centre frequency and amplitude (light blue: 3-8 Hz theta; yellow: 8-13 Hz alpha; orange: 13-18 Hz beta). **(D)** Number of fitted vs. simulated rhythmic components (spectral peaks), across all simulations and time points. The underestimation of the number of estimated spectral peaks is related to centre frequency: 3-8 Hz simulated peaks (blue) account for proportionally fewer of recovered peaks between 3-18 Hz (blue, yellow, orange) than from the other two tertiles. (Samples sizes by number of simulated peaks: 0 peaks = 798,753, 1 peak = 256,599, 2 peaks = 78,698, 3 peaks =14,790, 4 peaks = 1,160) **(E)** Model fit error is not affected by number of simulated peaks. Violin plots show the full sample distributions (white circle: median, blue box: first and third quartiles; whiskers: range).

Aperiodic and periodic fluctuations in resting-state EEG dynamics with eyes-closed, eyes-open behaviour (empirical data).

We ran logistics regression models to predict experimental condition with mean alpha power obtained from the Morlet wavelets analysis (see Methods). Results indicated that lower alpha power predicts the eyes-closed condition (β = -1.99, SE = 0.30, 95% CI [-2.61, -1.42]; Supplemental Table S1).

We fit additional regression models to predict the experimental condition (i.e., eyes-open vs. eyes-closed) from SPRiNT parameters. As discussed in the main text, mean alpha power, the standard deviation of alpha power, and mean aperiodic slope predicted experimental condition (i.e., eyes-open vs -closed; Supplemental Table S2). A Bayes factor analysis further supported

these findings, showcasing strong evidence for both the mean aperiodic slope and alpha power, but negative evidence (i.e., evidence for the null hypothesis) for the standard deviation of alpha power (Supplemental Figure S6). These results, along with effects reported using wavelets (above) replicate the well-documented decrease of alpha-band power in the eyes-open resting-state (compared to eyes-closed). Yet, spectral parameterization highlights the merits of tracking aperiodic activity, as SPRiNT captured an increase in aperiodic slope when participants closed their eyes. Similarly, SPRiNT captures dynamic changes in periodic power while simultaneously controlling for (and tracking) changes in the aperiodic component of the spectrogram, dissociating effects driven by changes by the aperiodic alone from changes in periodic power (Donoghue et al., 2020).

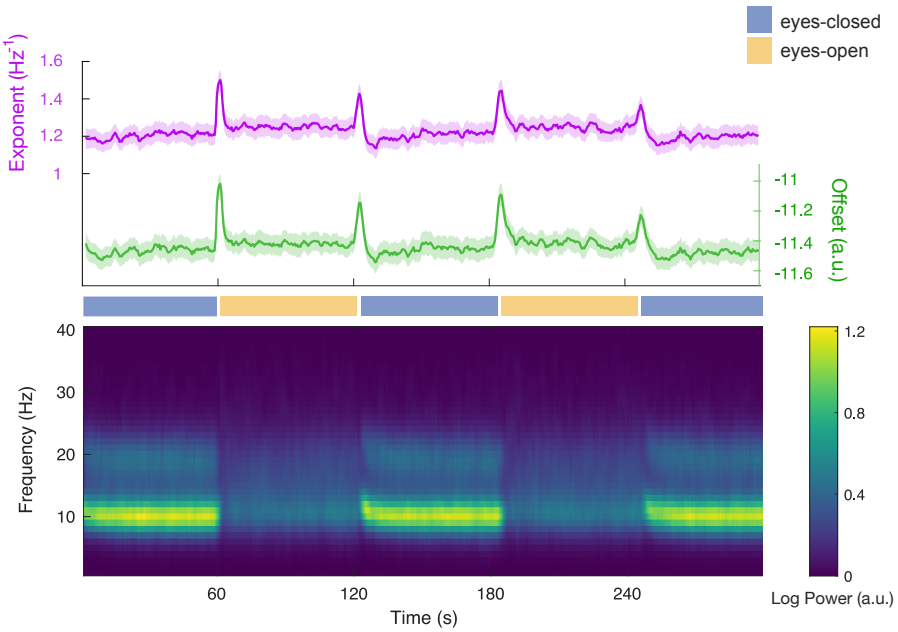

Figure S4. SPRiNT aperiodic parameters in resting-state EEG. SPRiNT aperiodic parameters (top panel; line: group mean (n = 178); shaded region: 95% CI) and SPRiNT periodic-activity averaged across participants (bottom panel).

		Condition	
Predictors	*Log-Odds*	*CI*	*p*
(Intercept)	-25.24	-33.08 – -17.95	**<0.001**
Alpha power (Morlet wavelets)	-1.99	-2.61 – -1.42	**<0.001**
Observations	356		
R^2 Tjur	0.140		

Table S1. Logistic regression model parameters for predicting condition (eyes-closed vs eyes-open) from the Morlet wavelet spectrograms, BF: 5.00×10^{-11}.

		Condition	
Predictors	*Log-Odds*	*CI*	*p*
(Intercept)	0.22	-3.75 – 4.25	0.913
mean center frequency	0.23	-0.06 – 0.52	0.119
std center frequency	-0.14	-1.02 – 0.74	0.761
mean alpha power	-6.57	-8.51 – -4.84	**<0.001**
std alpha power	5.43	1.62 – 9.46	**0.006**

mean aperiodic slope	2.52	1.52 – 3.59	**<0.001**
std aperiodic slope	-2.42	-8.22 – 3.76	0.424
Observations	356		
R^2 Tjur	0.424		

Table S2. Logistic regression model of SPRiNT parameters for predicting condition (eyes-closed vs eyes-open).

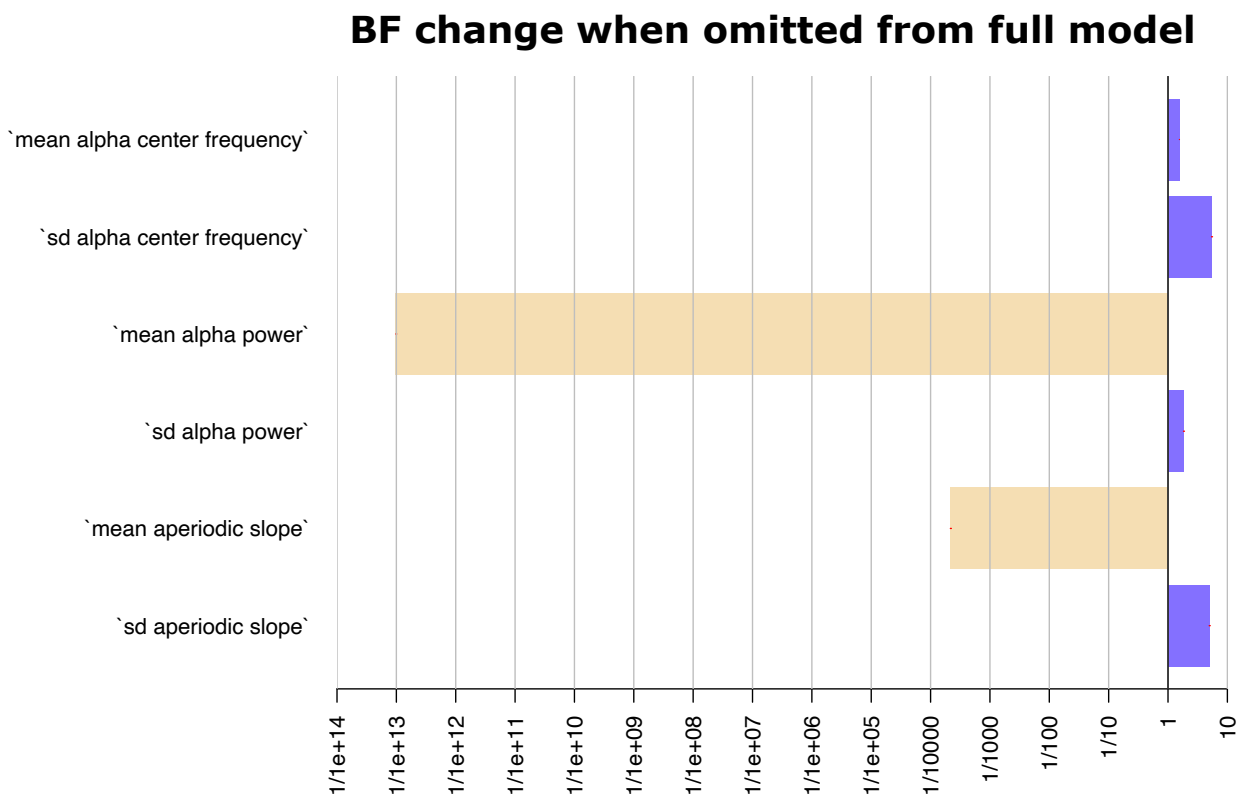

Figure S5. Bayes factor analysis for predicting experimental condition (eyes-open vs. eyes-closed). Bayes factor analysis of the linear regression models for predicting condition (eyes -open vs. eyes-closed) from resting-state brain activity. We compared evidence for the full model (see Methods) against reduced models where each predictor was removed sequentially (i.e., SPRiNT

parameter). Both the removal of mean alpha power and mean aperiodic slope had substantial negative effect on goodness of fit, with corresponding Bayes factors <1, which emphasizes their significance in accounting for the experimental condition (eyes-open vs. eyes-closed).

Prediction of biological age group from aperiodic and periodic spectral components of resting-state EEG (empirical data)

We used SPRiNT parameters obtained from both eyes-closed and eyes-open recordings to predict participants' age group (i.e., younger vs. older adults) in the LEMON dataset (Babayan et al., 2019). As discussed in the main text, the mean aperiodic slope and the standard deviation of alpha peak center frequency predicted the participants' age group for eyes-open resting-state recordings (Supplemental Table S3). A Bayes factor analysis provided strong evidence for mean aperiodic slope and substantial evidence for the standard deviation of alpha peak center frequency (Figure S7). Similarly, we found that mean aperiodic slope and mean alpha center frequency for eyes-closed resting-state recordings predicted the participants' age group (Supplemental Table S4). A Bayes factor analysis found strong and moderate evidence for mean aperiodic slope and mean alpha center frequency, respectively (Supplemental Figure S8). Taken together, these results suggest that SPRiNT parameters can predict significant participant demographic features (i.e., the aperiodic slope predicts age group in both the eyes-open and eyes-closed conditions).

We also ran the same regression analysis on alpha power extracted from wavelet spectrograms. Mean alpha power (6-14 Hz) predicted age group only in the eyes-closed condition ($\beta = -1.14$, SE = 0.38, 95% CI [-1.92, -0.41]; Table S6; for eyes-open, see Table S5). With SPRiNT, we demonstrated in main text that aperiodic slope and alpha mean center frequency were the strongest predictors of age group. We conclude that the effects identified with the wavelet

approach may be confounded by modulations of the aperiodic exponent, or a shift in alpha-peak power outside of a predefined band of interest, as one ages, as discussed by Donoghue et al. (2020) and Scally et al. (2018).

		Age	
Predictors	*Log-Odds*	*CI*	*p*
(Intercept)	2.25	-2.70 – 7.33	0.376
Eyes-open mean alpha center frequency	-0.06	-0.41 – 0.29	0.738
Eyes-open std alpha center frequency	1.27	0.24 – 2.35	**0.018**
Eyes-open mean alpha power	0.08	-3.04 – 2.93	0.957
Eyes-open std alpha power	-3.10	-8.38 – 1.96	0.237
Eyes-open mean aperiodic slope	-3.30	-4.85 – -1.90	**<0.001**
Eyes-open std aperiodic slope	2.95	-5.47 – 10.65	0.465
Observations	178		
R^2 Tjur	0.224		

Table S3. Eyes-open logistic regression model parameters for predicting age group, SPRiNT.

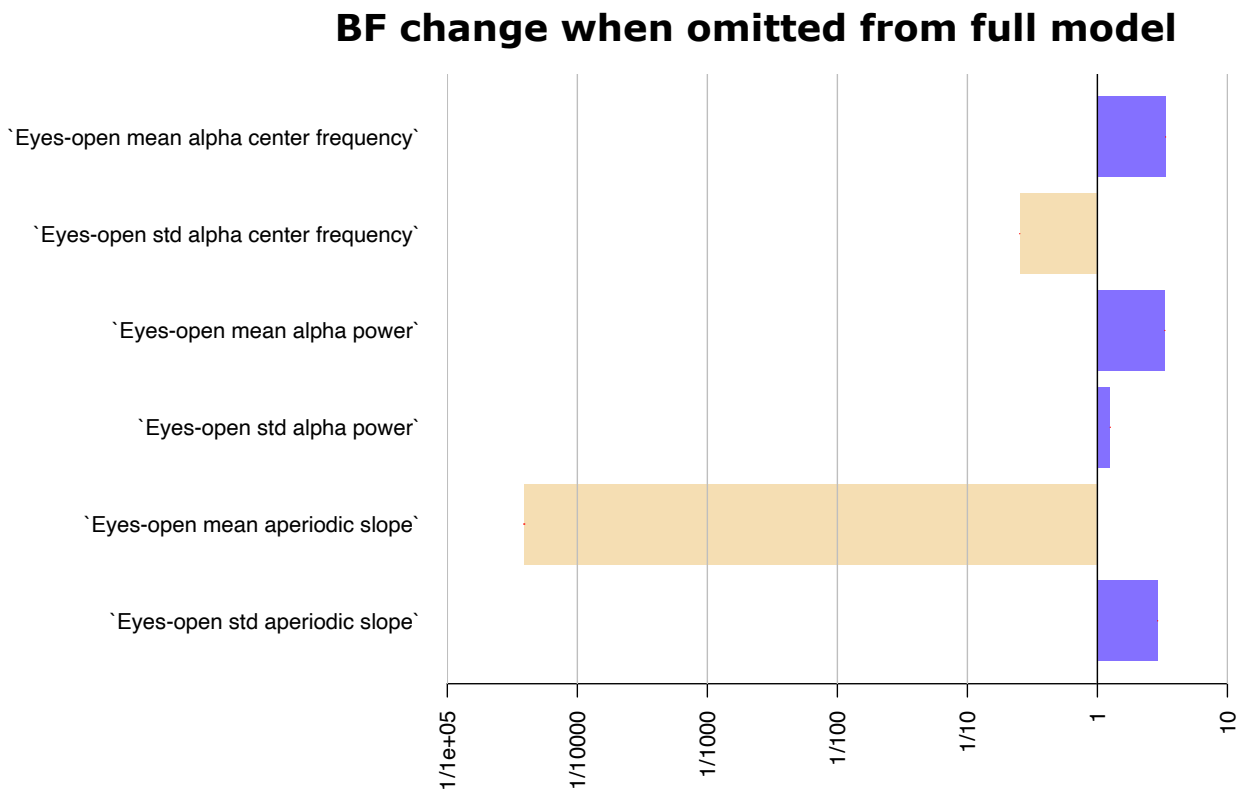

Figure S6. Bayes factor analysis for eyes-open resting-state brain activity.

Bayes factor analysis for the linear regression models for predicting age group from resting-state eyes-open brain activity. We compared evidence for the full model (see Methods) against reduced models where each predictor was removed sequentially (i.e., SPRiNT parameter). Both the removal of standard deviation of alpha center frequency and mean aperiodic slope had substantial negative effects on the goodness of fit, with corresponding Bayes factors <1, which emphasize their significance in accounting for age group.

		Age	
Predictors	*Log-Odds*	*CI*	*p*
(Intercept)	11.01	4.30 – 18.39	**0.002**
Eyes-closed mean center frequency	-0.68	-1.22 – -0.18	**0.010**
Eyes-closed std center frequency	0.59	-0.82 – 2.03	0.414
Eyes-closed mean alpha power	-0.26	-1.94 – 1.38	0.756
Eyes-closed std alpha power	-1.18	-6.19 – 3.72	0.638
Eyes-closed mean aperiodic slope	-4.25	-6.01 – -2.72	**<0.001**
Eyes-closed std aperiodic slope	1.98	-7.91 – 10.81	0.670
Observations	178		
R^2 Tjur	0. 259		

Table S4. Eyes-closed logistic regression model parameters for predicting age group, SPRiNT.

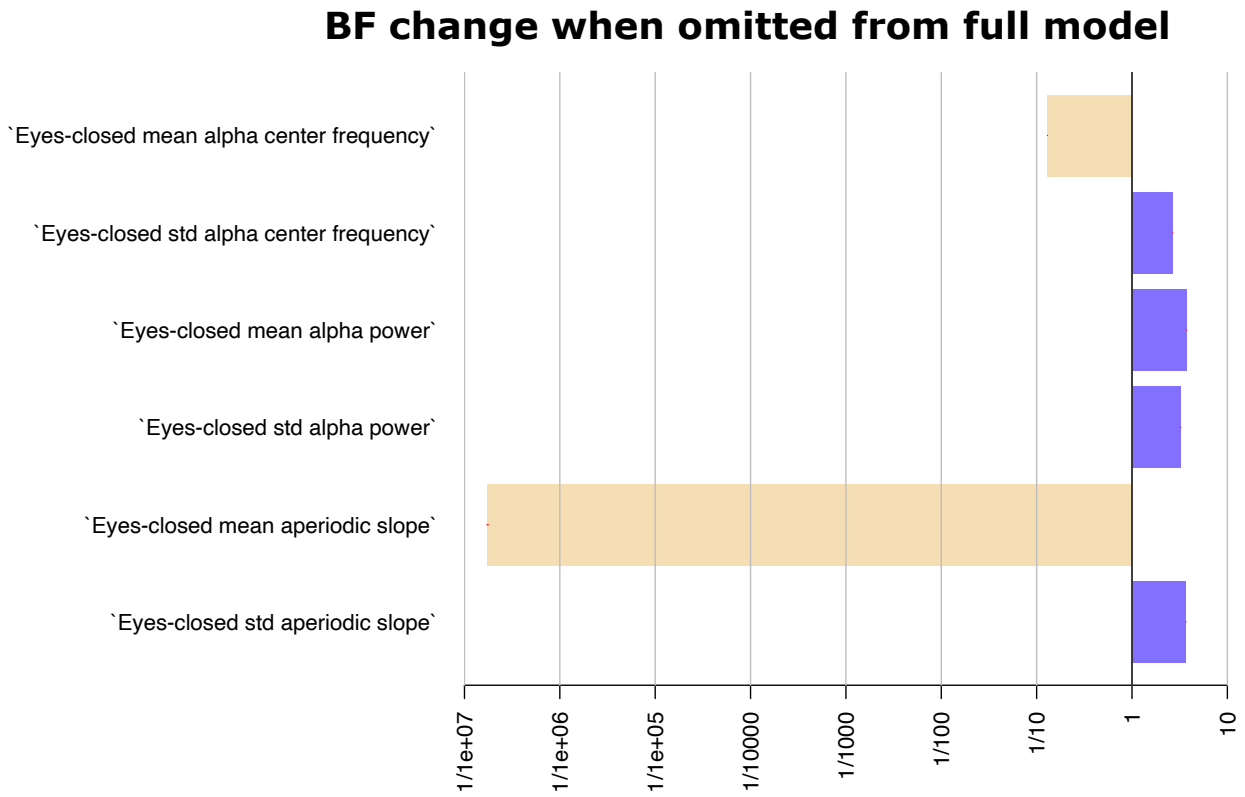

Figure S7. Bayes factor analysis for eyes-closed resting-state brain activity. Bayes factor analysis for the linear regression models predicting age group from resting-state eyes-closed brain activity. We compared evidence for the full model (see Methods) against reduced models where each predictor was removed sequentially (i.e., SPRiNT parameter). The removal of mean alpha center frequency and mean aperiodic slope had both substantial negative effects on the goodness of fit, with corresponding Bayes factor <1, which emphasize their significance in accounting for age group.

		Age	
Predictors	*Log-Odds*	*CI*	*p*
(Intercept)	-9.48	-22.17 – 2.67	0.133
Eyes-open alpha power (Morlet wavelets)	-0.68	-1.67 – 0.27	0.166
Observations	178		
R^2 Tjur	0.011		

Table S5. Eyes-open logistic regression model parameters for predicting age group, Morlet wavelets (BF = 2.50).

		Age	
Predictors	*Log-Odds*	*CI*	*p*
(Intercept)	-15.02	-24.83 – -5.93	**0.002**
Eyes-closed alpha power (Morlet wavelets)	-1.14	-1.92 – -0.41	**0.003**
Observations	178		
R^2 Tjur	0.053		

Table S6. Eyes-closed logistic regression model parameters for predicting age group, Morlet wavelet spectrogram (BF = 0.07).

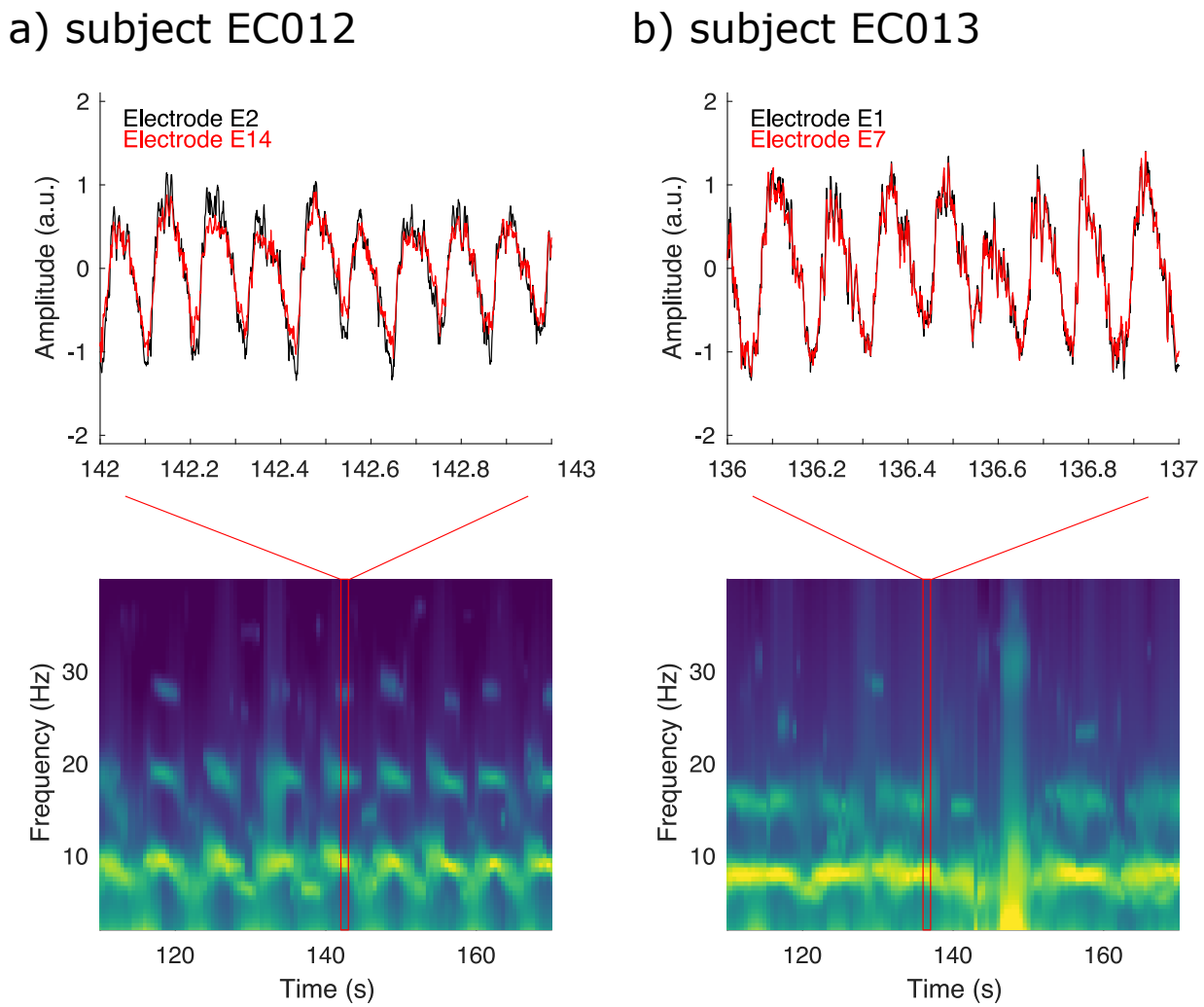

Figure S8. Examples of sawtooth rhythms from two representative electrodes in entorhinal cortex layer 3 from both subjects. (A) Example time-series of prominent sawtooth rhythms from two representative electrodes during a movement bout for subject EC012 (top), producing harmonics of activity in the average modelled spectrogram (bottom). (**B**) Same as (A), for subject EC013.

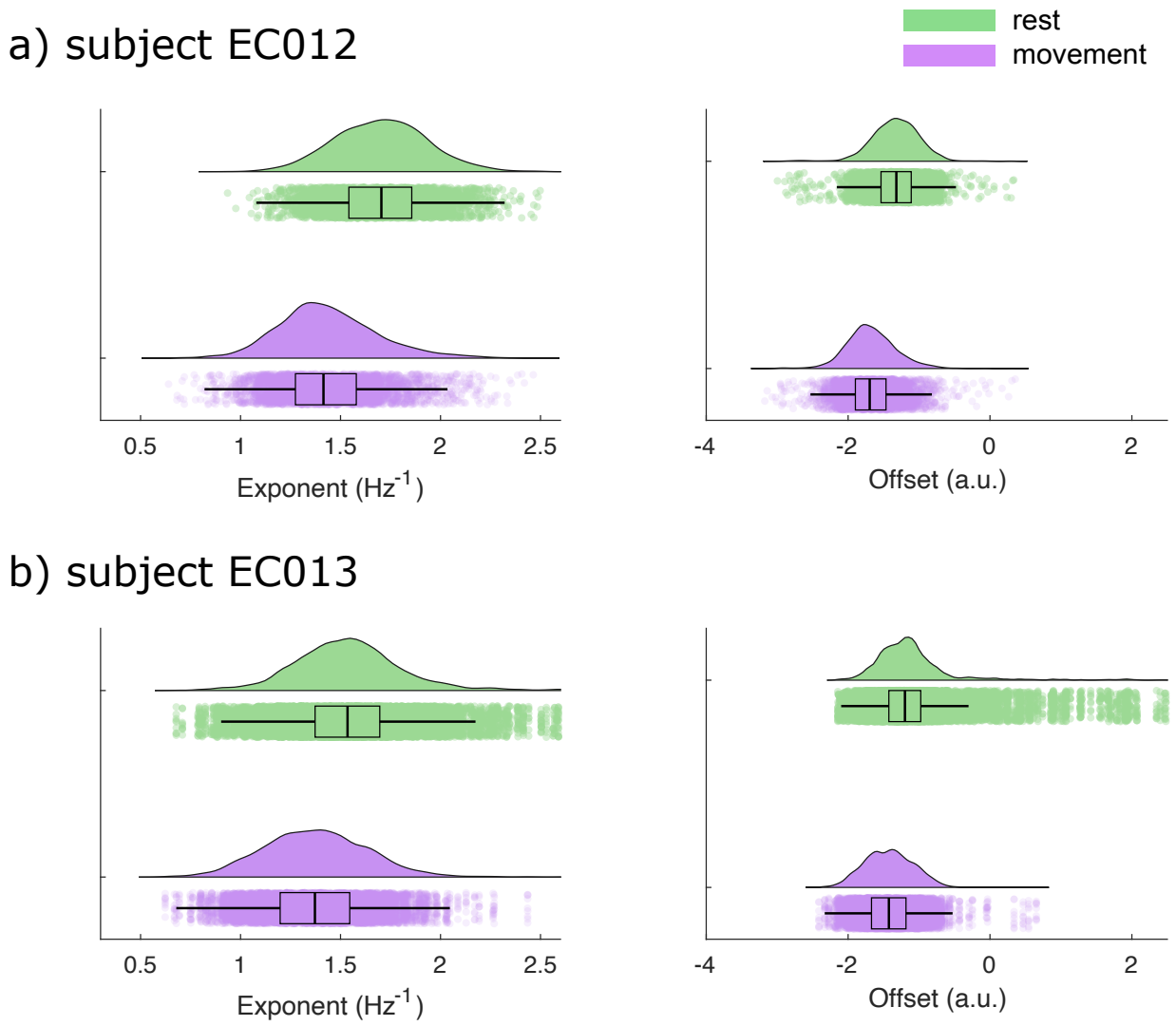

208

209 **Figure S9. Empirical distributions of SPRiNT aperiodic exponent and offset parameters. (A)**
210 Empirical distributions of aperiodic exponent and offset estimates for subject EC012 at time bins
211 associated with rest (green) and movement (purple) bouts (boxplot line: median; boxplot limits:
212 first and third quartiles; whiskers: range). **(B)** Same as (A), for subject EC013. Sample sizes:
213 EC012 rest (movement) = 3,896 (4,584) bins; EC013 rest (movement) = 20,970 (10,386) bins.

214

215

216

References

Babayan, A., Erbey, M., Kumral, D., Reinelt, J. D., Reiter, A. M. F., Röbbig, J., . . . Villringer, A. (2019). A mind-brain-body dataset of MRI, EEG, cognition, emotion, and peripheral physiology in young and old adults. *Scientific Data*, *6*(1), 180308. doi:10.1038/sdata.2018.308

Donoghue, T., Haller, M., Peterson, E. J., Varma, P., Sebastian, P., Gao, R., . . . Knight, R. T. (2020). Parameterizing neural power spectra into periodic and aperiodic components. *Nature Neuroscience, 23*(12), 1655-1665. doi:10.1038/s41593-020-00744-x

Donoghue, T., Schaworonkow, N., & Voytek, B. (2021). Methodological considerations for studying neural oscillations. *Eur J Neurosci*. doi:10.1111/ejn.15361

Scally, B., Burke, M. R., Bunce, D., & Delvenne, J.-F. (2018). Resting-state EEG power and connectivity are associated with alpha peak frequency slowing in healthy aging. *Neurobiology of Aging*, *71*, 149-155. doi:10.1016/j.neurobiolaging.2018.07.004